
Preserving Differential Privacy in Adversarial Learning with Provable Robustness

NhatHai Phan

NJIT
Newark, New Jersey, USA
phan@njit.edu

My T. Thai

University of Florida
Gainesville, Florida, USA
mythai@cise.ufl.edu

Ruoming Jin

Kent State University
Kent, Ohio, USA
rjin1@kent.edu

Han Hu

NJIT
Newark, New Jersey, USA
hh255@njit.edu

Dejing Dou

University of Oregon
Eugene, OR, USA
dou@cs.uoregon.edu

Abstract

In this paper, we aim to develop a novel mechanism to preserve differential privacy (**DP**) in adversarial learning for deep neural networks, with *provable robustness to adversarial examples*. We leverage the sequential composition theory in differential privacy, to establish a new connection between differential privacy preservation and provable robustness. To address the trade-off among model utility, privacy loss, and robustness, we design an original, differentially private, adversarial objective function, based on the post-processing property in DP, to tighten the sensitivity of our model. Theoretical analysis and thorough evaluations show that our mechanism notably improves the robustness of DP deep neural networks.

1 Introduction

In spite of advantages in terms of application utility, the pervasiveness of machine learning exposes new vulnerabilities in software systems. Adversaries can conduct devastating attacks, in which deployed machine learning models can be used (a) to reveal sensitive information in private training data [1–4], and/or (b) to make the models misclassify, such as *adversarial examples* [5–7]. Efforts to prevent such devastating attacks typically seek one of three solutions: **(1)** Models which preserve differential privacy (**DP**) [16], a rigorous cryptography-based formulation of privacy in probabilistic terms, thereby preventing revelation of sensitive information about the subjects involved in the training data [8, 9]; **(2)** Adversarial training algorithms, which augment training data to consist of benign examples and adversarial examples crafted during the training process, thereby empirically increasing the classification accuracy given adversarial examples [4, 10–12]; and **(3)** Provable robustness, in which the model classification given adversarial examples is theoretically guaranteed to be consistent, i.e., a small perturbation in the input does not change the predicted label [13–15].

On one hand, *private models*, trained with existing privacy-preserving mechanisms, are unshielded under adversarial examples. On the other hand, *robust models*, trained with adversarial learning algorithms (with or without provable robustness to adversarial examples), do not offer privacy protections to the training data. That poses serious risks to machine learning-based systems in critical applications, e.g., face recognition, health care, etc.; since adversaries can attack a deployed model by using both privacy inference attacks [1–4] and adversarial examples [5–7]. To be assured, a model must be *i) private to protect the training data, and ii) robust to adversarial examples*. There is an urgent demand to train such a secure model with a high utility. Unfortunately, there has not yet been research on how to develop such a model, which thus remains a largely open challenge.

Simply combining existing DP-preserving mechanisms [8, 21–24] and provable robustness conditions [13–15] cannot solve the problem, for many reasons. **(a)** Existing sensitivity bounds [22–24] and designs [8, 21] have not been developed to protect the training data in adversarial training. It is obvious that the adversarial examples usually are very similar to the benign examples. Therefore, using adversarial examples crafted from the private training data to train our models introduces a previously unknown privacy risk, disclosing the participation of the benign examples. **(b)** There is an unrevealed interplay between DP preservation and robustness bounds. **(c)** Existing algorithms [8, 13–15, 21–24] cannot be readily applied to address the trade-off among model utility, privacy loss, and robustness. Therefore, theoretically bounding the robustness of a model (which both protects the privacy and is robust against adversarial examples) is nontrivial.

Our Contributions. Motivated by this open problem, we propose to develop a novel *differentially private adversarial learning (DPAL)* mechanism to: **1)** preserve DP of the training data, **2)** be provably and practically robust to adversarial examples, and **3)** retain high model utility. In our mechanism, privacy-preserving noise is injected into inputs and hidden layers to achieve DP in learning private model parameters (**Theorem 1**). Then, we incorporate ensemble adversarial learning into our mechanism to improve the decision boundary under DP protections. To do this, we introduce a concept of *DP adversarial examples*, which are crafted using benign examples in the private training data under DP guarantees (**Eq. 10**). To address the trade-off between model utility and privacy loss, we propose a new DP adversarial objective function to tighten the model’s global sensitivity (**Theorem 2**); thus, we significantly reduce the amount of noise injected into our function in learning DP model parameters, compared with existing works [22–24].

After preserving DP in learning model parameters, we focus on establishing a solid theoretical and practical connection among privacy preservation, adversarial learning, and provable robustness. Noise injected into different layers is considered as a sequence of randomizing mechanisms, providing different levels of robustness. By leveraging the *sequential composition theory* in DP [17], we derive a novel generalized robustness bound, which essentially is a composition of these levels of robustness (**Theorem 3** and **Proposition 1**). To our knowledge, our mechanism establishes the first connection between *DP preservation to protect the training data* and *provable robustness against adversarial examples* in deep learning. Such a mechanism will greatly extend the applicability of machine learning, by fortifying the models in both privacy and security aspects. Rigorous experiments conducted on MNIST and CIFAR-10 datasets [18, 19] show that our mechanism notably enhances the robustness of DP deep neural networks.

2 Background and Problem Definition

In this section, we revisit adversarial learning, DP, and introduce our problem definition. Let D be a database that contains N tuples, each of which contains data $x \in [-1, 1]^d$ and a *ground-truth label* $y \in \mathbb{Z}_K$, with K possible categorical outcomes. Each y is a one-hot vector of K categories $y = \{y_1, \dots, y_K\}$. A single *true class label* $y_x \in y$ given $x \in D$ is assigned to only one of the K categories. On input x and parameters θ , a model outputs class scores $f : \mathbb{R}^d \rightarrow \mathbb{R}^K$ that maps d -dimensional inputs x to a vector of scores $f(x) = \{f_1(x), \dots, f_K(x)\}$ s.t. $\forall k \in [1, K] : f_k(x) \in [0, 1]$ and $\sum_{k=1}^K f_k(x) = 1$. The class with the highest score value is selected as the *predicted label* for the data tuple, denoted as $y(x) = \max_{k \in K} f_k(x)$. A loss function $L(f(x), y)$ presents the penalty for mismatching between the predicted values $f(x)$ and original values y . The notations and terminologies frequently used in this paper are summarized in Table 1, located in **Appendix A**. Let us briefly revisit DP and DP-preserving techniques in deep learning, starting with the definition of DP.

Definition 1 (ϵ, δ) -DP [16]. A randomized algorithm A fulfills (ϵ, δ) -DP, if for any two databases D and D' differing at most one tuple, and for all $O \subseteq \text{Range}(A)$, we have:

$$\Pr[A(D) = O] \leq e^\epsilon \Pr[A(D') = O] + \delta \quad (1)$$

Here, ϵ controls the amount by which the distributions induced by D and D' may differ, δ is a broken probability. DP also applies to general metrics $\rho(D, D') \leq 1$, where ρ can be a Hamming metric as in Definition 1 and l_p -norms [20]. DP-preserving algorithms in deep learning can be categorized into two lines: 1) introducing noise into *gradients* of parameters [8, 21], and 2) injecting noise into objective functions [22–24]. In Lemmas 2 and 4, we will show that our mechanism achieves better sensitivity bounds compared with existing works [22–24].

Adversarial Learning. For some target model f and inputs (x, y_x) , the adversary’s goal is to find an *adversarial example* $x^{\text{adv}} = x + \alpha$, where α is the perturbation introduced by the attacker, such

that: (1) x^{adv} and x are close, and (2) the model misclassifies x^{adv} , i.e., $y(x^{\text{adv}}) \neq y(x)$. In this paper, we consider well-known $l_p \in \{1, 2, \infty\}$ -norm bounded attacks [5]. Let $l_p(\mu) = \{\alpha \in \mathbb{R}^d : \|\alpha\|_p \leq \mu\}$ be the l_p -norm ball of radius μ . One of the goals in adversarial learning is to minimize the risk over adversarial examples: $\theta^* = \arg \min_{\theta} \mathbb{E}_{(x, y_{\text{true}}) \sim \mathcal{D}} [\max_{\|\alpha\|_p \leq \mu} L(f(x + \alpha, \theta), y_x)]$, where an attack is used to approximate solutions to the inner maximization problem, and the outer minimization problem corresponds to training the model f with parameters θ over these adversarial examples $x^{\text{adv}} = x + \alpha$. There are two basic adversarial example attacks. The first one is a *single-step* algorithm, in which only a single gradient computation is required. For instance, **FGSM** algorithm [5] finds adversarial examples by solving the inner maximization $\max_{\|\alpha\|_p \leq \mu} L(f(x + \alpha, \theta), y_x)$. The second one is an *iterative* algorithm, in which multiple gradients are computed and updated. For instance, in [25], FGSM is applied multiple times with T_μ small steps, each of which has a size of μ/T_μ .

To improve the robustness of models, prior work focused on two directions: 1) Producing correct predictions on adversarial examples, while not compromising the accuracy on legitimate inputs [10–12, 26–30]; and 2) Detecting adversarial examples, without introducing too many false positives [31–35]. Among existing solutions, adversarial training appears to hold the greatest promise for learning robust models [36]. One of the well-known algorithms was proposed in [37]. At every training step, new adversarial examples are generated and injected into batches containing both benign and adversarial examples. The pseudo-code of this algorithm [37] is provided in **Appendix B**.

DP and Provable Robustness. Recently, some algorithms [13] have been proposed to derive provable robustness, in which each prediction is guaranteed to be consistent under the perturbation α , if a robustness condition is held. Given a benign example x , we focus on achieving a robustness condition to attacks of $l_p(\mu)$ -norm, as follows:

$$\forall \alpha \in l_p(\mu) : f_k(x + \alpha) > \max_{i: i \neq k} f_i(x + \alpha) \quad (2)$$

where $k = y(x)$, indicating that a small perturbation α in the input does not change the predicted label $y(x)$. To achieve the robustness condition in Eq. 2, Lecuyer et al. [38] introduce an algorithm, called **PixelDP**. By considering an input x (e.g., images) as databases in DP parlance, and individual features (e.g., pixels) as tuples, PixelDP shows that randomizing the scoring function $f(x)$ to enforce DP on a small number of pixels in an image guarantees robustness of predictions against adversarial examples. To randomize $f(x)$, *random noise* σ_r is injected into either input x or an arbitrary hidden layer, resulting in the following (ϵ_r, δ_r) -PixelDP condition:

Lemma 1 (ϵ_r, δ_r) -PixelDP [38]. *Given a randomized scoring function $f(x)$ satisfying (ϵ_r, δ_r) -PixelDP w.r.t. a l_p -norm metric, we have:*

$$\forall k, \forall \alpha \in l_p(1) : \mathbb{E} f_k(x) \leq e^{\epsilon_r} \mathbb{E} f_k(x + \alpha) + \delta_r \quad (3)$$

where $\mathbb{E} f_k(x)$ is the expected value of $f_k(x)$, ϵ_r is a predefined budget, and δ_r is a broken probability.

At the prediction time, a certified robustness check is implemented for each prediction. A generalized robustness condition is proposed as follows:

$$\hat{\mathbb{E}}_{lb} f_k(x) > e^{2\epsilon_r} \max_{i: i \neq k} \hat{\mathbb{E}}_{ub} f_i(x) + (1 + e^{\epsilon_r}) \delta_r \quad (4)$$

where $\hat{\mathbb{E}}_{lb}$ and $\hat{\mathbb{E}}_{ub}$ are the lower and upper bounds of the expected value $\hat{\mathbb{E}} f(x) = \frac{1}{n} \sum_n f(x)_n$, derived from the Monte Carlo estimation with an η -confidence, given n is the number of invocations of $f(x)$ with independent draws in the noise σ_r . Passing the check for a given input guarantees that no perturbation exists up to $l_p(1)$ -norm, that causes the model to change its prediction. In other words, the classification model, based on $\hat{\mathbb{E}} f(x)$, i.e., $\arg \max_k \hat{\mathbb{E}} f_k(x)$, is provably robust to attacks of $l_p(1)$ -norm on input x with probability $\geq \eta$. PixelDP does not preserve DP in learning private parameters θ to protect the training data [38]. That is different from our goal.

3 DPAL with Provable Robustness

Our new DP-preserving mechanism, called DPAL, is presented in Alg. 2 (**Appendix C**). Our network can be represented as: $f(x) = g(a(x, \theta_1), \theta_2)$, where $a(x, \theta_1)$ is a feature representation learning model with x as an input, and g will take the output of $a(x, \theta_1)$ and return the class scores $f(x)$. At a

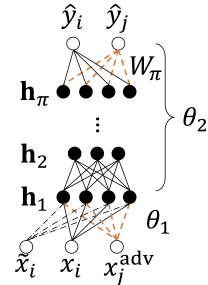


Figure 1: An instance of DPAL.

high level, DPAL has three key components: **(1)** DP $a(x, \theta_1)$, which is to preserve DP in learning the feature representation model $a(x, \theta_1)$; **(2)** DP Adversarial Learning, which focuses on preserving DP in adversarial learning, given DP $a(x, \theta_1)$; and **(3)** Provable Robustness and Verified Inferring, which are to compute robustness bounds given an input at the inference time. In particular, given a deep neural network f with model parameters θ (Lines 1-2), the network is trained over T random training batches B_t ($t \in [1, T]$). Each B_t is a set of m training examples $x_i \in D$ (Lines 4-15).

DP Feature Representation Learning. Our idea is to use auto-encoder to simultaneously learn DP parameters θ_1 and ensure that the output of $a(x, \theta_1)$ is DP. The reasons we choose an auto-encoder are: (1) It is easier to train, given its small size; and (2) It can be reused for different predictive models. Figure 1 shows the structure of our network. We use a data reconstruction function (cross-entropy), given a batch B_t of the input x_i , as follows:

$$\mathcal{R}_{B_t}(\theta_1) = \sum_{x_i \in B_t} \sum_{j=1}^d \left[x_{ij} \log(1 + e^{-\theta_{1j} h_i}) + (1 - x_{ij}) \log(1 + e^{\theta_{1j} h_i}) \right] \quad (5)$$

where the affine transformation of x_i is $h_i = \theta_1^T x_i$, the hidden layer \mathbf{h}_1 of $a(x, \theta_1)$ given the batch B_t is denoted as $\mathbf{h}_{1B_t} = \{\theta_1^T x_i\}_{x_i \in B_t}$, and $\tilde{x}_i = \theta_1 h_i$ is the reconstruction of x_i .

To preserve ϵ_1 -DP in learning θ_1 where ϵ_1 is a privacy budget, we first derive the 1st-order polynomial approximation of $\mathcal{R}_{B_t}(\theta_1)$ by applying Taylor Expansion [39], denoted as $\tilde{\mathcal{R}}_{B_t}(\theta_1)$. Then, *Functional Mechanism* [40] is employed to inject noise into coefficients of the approximated function $\tilde{\mathcal{R}}_{B_t}(\theta_1)$.

$$\tilde{\mathcal{R}}_{B_t}(\theta_1) = \sum_{x_i \in B_t} \sum_{j=1}^d \sum_{l=1}^2 \sum_{r=0}^1 \frac{\mathbf{F}_{lj}^{(r)}(0)}{r!} (\theta_{1j} h_i)^r \quad (6)$$

where $\mathbf{F}_{1j}(z) = x_{ij} \log(1 + e^{-z})$, $\mathbf{F}_{2j}(z) = (1 - x_{ij}) \log(1 + e^z)$, we have that: $\tilde{\mathcal{R}}_{B_t}(\theta_1) = \sum_{x_i \in B_t} \sum_{j=1}^d \left[\log 2 + \theta_{1j} \left(\frac{1}{2} - x_{ij} \right) h_i \right]$. In $\tilde{\mathcal{R}}_{B_t}(\theta_1)$, parameters θ_{1j} derived from the function optimization need to be ϵ_1 -DP. To achieve that, Laplace noise $\frac{1}{m} \text{Lap}(\frac{\Delta_{\mathcal{R}}}{\epsilon_1})$ is injected into coefficients $\left(\frac{1}{2} - x_{ij} \right) h_i$, where $\Delta_{\mathcal{R}}$ is the sensitivity of $\tilde{\mathcal{R}}_{B_t}(\theta_1)$, as follows (log 2 can be ignored):

$$\tilde{\mathcal{R}}_{B_t}(\theta_1) = \sum_{x_i \in B_t} \sum_{j=1}^d \left[\theta_{1j} \left(\left(\frac{1}{2} - x_{ij} \right) h_i + \frac{1}{m} \text{Lap}(\frac{\Delta_{\mathcal{R}}}{\epsilon_1}) \right) \right] = \sum_{x_i \in B_t} \left[\sum_{j=1}^d \left(\frac{1}{2} \theta_{1j} \bar{h}_i - x_i \tilde{x}_i \right) \right] \quad (7)$$

To ensure that the computation of \tilde{x}_i does not access the original data, we further inject Laplace noise $\frac{1}{m} \text{Lap}(\frac{\Delta_{\mathcal{R}}}{\epsilon_1})$ into x_i (Line 6). The perturbed function now becomes:

$$\bar{\mathcal{R}}_{B_t}(\theta_1) = \sum_{x_i \in B_t} \left[\sum_{j=1}^d \left(\frac{1}{2} \theta_{1j} \bar{h}_i - \bar{x}_i \tilde{x}_i \right) \right] \quad (8)$$

where $\bar{x}_i = x_i + \frac{1}{m} \text{Lap}(\frac{\Delta_{\mathcal{R}}}{\epsilon_1})$, $h_i = \theta_1^T \bar{x}_i$, $\bar{h}_i = h_i + \frac{2}{m} \text{Lap}(\frac{\Delta_{\mathcal{R}}}{\epsilon_1})$, and $\tilde{x}_i = \theta_1 \bar{h}_i$ (Lines 3 and 6). Let us denote β as the number of hidden neurons in \mathbf{h}_1 ; h_i is bounded in $[-1, 1]$ to compute the global sensitivity $\Delta_{\mathcal{R}}$ as follows:

Lemma 2 *The global sensitivity of $\tilde{\mathcal{R}}$ over any two neighboring batches, B_t and B'_t , is as follows: $\Delta_{\mathcal{R}} \leq d(\beta + 2)$.*

By setting $\Delta_{\mathcal{R}} = d(\beta + 2)$, we show that the Alg. 2 achieves ϵ_1 -DP in the following Theorem.

Theorem 1 *Algorithm 2 preserves ϵ_1 -DP in learning θ_1 .*

Detailed proofs of all the Lemmas and Theorems can be found in the Appendices. After achieving ϵ_1 -DP in learning θ_1 , we further show that the output of $a(x, \theta_1)$, which is the perturbed affine transformation $\bar{\mathbf{h}}_{1B_t} = \{\bar{\theta}_1^T \bar{x}_i + \frac{2}{m} \text{Lap}(\frac{\Delta_{\mathcal{R}}}{\epsilon_1})\}_{x_i \in B_t}$, is (ϵ_1/γ) -DP, given $\gamma = \frac{2\Delta_{\mathcal{R}}}{m\|\bar{\theta}_1\|_{1,1}}$ and $\|\bar{\theta}_1\|_{1,1}$ is the maximum 1-norm of θ_1 's columns [41]. This is important to tighten the privacy budget consumption in computing the remaining hidden layers $g(a(x, \theta_1), \theta_2)$. In fact, without using additional information from the original data, the computation of $g(a(x, \theta_1), \theta_2)$ is also (ϵ_1/γ) -DP, i.e., thanks to the post-processing property of DP. We have the following Lemma.

Lemma 3 *Algorithm 2 preserves (ϵ_1/γ) -DP in computing the affine transformation $\bar{\mathbf{h}}_{1B_t}$.*

DP Adversarial Learning. To integrate adversarial learning, we first draft adversarial examples x_j^{adv} using benign examples x_j , with an ensemble of attack algorithms A and a random perturbation budget $\mu_t \in (0, 1]$, at each step t (Lines 8-13). Adversarial examples (crafted from the training data) are very similar to the original benign examples. That clearly poses privacy risks. Therefore, x_j^{adv} is perturbed to ensure DP in the training procedure, as follows:

$$\bar{x}_j^{\text{adv}} = x_j^{\text{adv}} + \frac{1}{m} \text{Lap}\left(\frac{\Delta \mathcal{R}}{\epsilon_1}\right), \text{ where } x_j^{\text{adv}} = x_j + \mu \cdot \text{sign}\left(\nabla_{x_j} \mathcal{L}(f(x_j, \theta), y(x_j))\right) \quad (9)$$

where $y(x_j)$ is the class prediction result of $f(x_j)$ to avoid label leaking of the benign examples x_j during the adversarial example crafting. Similar to x_j , training the auto-encoder with adversarial examples \bar{x}_j^{adv} , i.e., $a(\bar{x}_j^{\text{adv}}, \theta_1)$, preserves ϵ_1 -DP. It can be extended to iterative attacks as follows:

$$\bar{x}_{j,0}^{\text{adv}} = x_j, \bar{x}_{j,t+1}^{\text{adv}} = \bar{x}_{j,t}^{\text{adv}} + \frac{\mu}{T_\mu} \cdot \text{sign}\left(\nabla_{\bar{x}_{j,t}^{\text{adv}}} \mathcal{L}(f(\bar{x}_{j,t}^{\text{adv}}, \theta), y(\bar{x}_{j,t}^{\text{adv}}))\right), \bar{x}_{j,T_\mu}^{\text{adv}} = \bar{x}_{j,T_\mu}^{\text{adv}} + \frac{1}{m} \text{Lap}\left(\frac{\Delta \mathcal{R}}{\epsilon_1}\right) \quad (10)$$

where $y(\bar{x}_{j,t}^{\text{adv}})$ is the prediction result of $f(\bar{x}_{j,t}^{\text{adv}}, \theta)$, and $t \in [0, T_\mu - 1]$.

Second, we propose a novel DP adversarial objective function $L_{B_t}(\theta_2)$, in which the loss function \mathcal{L} for benign examples is combined with an additional loss function Υ for DP adversarial examples, to optimize the parameters θ_2 . The objective function $L_{B_t}(\theta_2)$ is defined as follows:

$$L_{B_t}(\theta_2) = \frac{1}{m(1 + \xi)} \left(\sum_{\bar{x}_i \in \bar{B}_t} \mathcal{L}(f(\bar{x}_i, \theta_2), y_i) + \xi \sum_{\bar{x}_j^{\text{adv}} \in \bar{B}_t^{\text{adv}}} \Upsilon(f(\bar{x}_j^{\text{adv}}, \theta_2), y_j) \right) \quad (11)$$

where ξ is a hyper-parameter. For the sake of clarity, in Eq. 11, we denote y_i and y_j as the true class labels y_{x_i} and y_{x_j} of examples x_i and x_j . Note that \bar{x}_j^{adv} and x_j share the same label y_{x_j} . \bar{B}_t and \bar{B}_t^{adv} are sets of perturbed inputs \bar{x}_i and DP adversarial examples \bar{x}_j^{adv} .

Now we are ready to preserve DP in objective functions $\mathcal{L}(f(\bar{x}_i, \theta_2), y_i)$ and $\Upsilon(f(\bar{x}_j^{\text{adv}}, \theta_2), y_j)$ in order to achieve DP in learning θ_2 . Since the objective functions use the true class labels y_i and y_j , we need to protect the labels at the output layer. Let us first present our approach to preserve DP in the objective function \mathcal{L} for benign examples. Given $\mathbf{h}_{\pi i}$ computed from the \bar{x}_i through the network with W_π is the parameter at the last hidden layer \mathbf{h}_π . Cross-entropy function can be applied as follows:

$$\begin{aligned} \mathcal{L}_{\bar{B}_t}(\theta_2) &= \sum_{\bar{x}_i \in \bar{B}_t} \mathcal{L}(f(\bar{x}_i, \theta_2), y_i) = - \sum_{k=1}^K \sum_{\bar{x}_i} \left[y_{ik} \log(1 + e^{-\mathbf{h}_{\pi i} W_{\pi k}}) + (1 - y_{ik}) \log(1 + e^{\mathbf{h}_{\pi i} W_{\pi k}}) \right] \\ &\cong \sum_{k=1}^K \sum_{\bar{x}_i} \left[\mathbf{h}_{\pi i} W_{\pi k} - (\mathbf{h}_{\pi i} W_{\pi k}) y_{ik} + \log(1 + e^{-\mathbf{h}_{\pi i} W_{\pi k}}) \right] \end{aligned}$$

By applying Taylor Expansion, the term $\log(1 + e^{-\mathbf{h}_{\pi i} W_{\pi k}})$ can be approximated as a 2nd-order polynomial function:

$$\mathcal{L}_{\bar{B}_t}(\theta_2) \cong \sum_{k=1}^K \sum_{\bar{x}_i} \left[\mathbf{h}_{\pi i} W_{\pi k} - (\mathbf{h}_{\pi i} W_{\pi k}) y_{ik} - \frac{1}{2} |\mathbf{h}_{\pi i} W_{\pi k}| + \frac{1}{8} (\mathbf{h}_{\pi i} W_{\pi k})^2 \right] = \mathcal{L}_{1\bar{B}_t}(\theta_2) - \mathcal{L}_{2\bar{B}_t}(\theta_2)$$

where $\mathcal{L}_{1\bar{B}_t}(\theta_2) = \sum_{k=1}^K \sum_{\bar{x}_i} [\mathbf{h}_{\pi i} W_{\pi k} - \frac{1}{2} |\mathbf{h}_{\pi i} W_{\pi k}| + \frac{1}{8} (\mathbf{h}_{\pi i} W_{\pi k})^2]$, and $\mathcal{L}_{2\bar{B}_t}(\theta_2) = \sum_{k=1}^K \sum_{\bar{x}_i} (\mathbf{h}_{\pi i} y_{ik}) W_{\pi k}$.

Based on the *post-processing property of DP* [17], $\mathbf{h}_{\pi \bar{B}_t} = \{\mathbf{h}_{\pi i}\}_{\bar{x}_i \in \bar{B}_t}$ is (ϵ_1/γ) -DP, since the computation of $\bar{\mathbf{h}}_{1\bar{B}_t}$ is (ϵ_1/γ) -DP (Lemma 3). As a result, we have that: 1) The optimization of the function $\mathcal{L}_{1\bar{B}_t}(\theta_2)$ does not disclose any information from the training data; and 2) $\frac{\text{Pr}(\mathcal{L}_{1\bar{B}_t}(\theta_2))}{\text{Pr}(\mathcal{L}_{1\bar{B}_t'}(\theta_2))} = \frac{\text{Pr}(\mathbf{h}_{\pi \bar{B}_t})}{\text{Pr}(\mathbf{h}_{\pi \bar{B}_t'})} \leq e^{\epsilon_1/\gamma}$, given any two neighboring batches \bar{B}_t and \bar{B}_t' . Thus, to preserve DP in $\mathcal{L}_{\bar{B}_t}(\theta_2)$, we only need to preserve ϵ_2 -DP in the function $\mathcal{L}_{2\bar{B}_t}(\theta_2)$, which accesses the ground-truth label y_{ik} . Given coefficients $\mathbf{h}_{\pi i} y_{ik}$, the sensitivity $\Delta_{\mathcal{L}_2}$ of $\mathcal{L}_{2\bar{B}_t}(\theta_2)$ is computed as:

Lemma 4 Let \bar{B}_t and \bar{B}_t' be neighboring batches of benign examples, we have the following inequality: $\Delta_{\mathcal{L}_2} \leq 2|\mathbf{h}_\pi|$, where $|\mathbf{h}_\pi|$ is the number of hidden neurons in \mathbf{h}_π .

The sensitivity of our objective function is notably smaller than the state-of-the-art bound, which is $K(|\mathbf{h}_\pi| + \frac{1}{4}|\mathbf{h}_\pi|^2)$ [24]. This is crucial to improve our model utility under strong attacks, while providing the same level of DP protections. The perturbed functions are as follows:

$$\bar{\mathcal{L}}_{\bar{B}_t}(\theta_2) = \mathcal{L}_{1\bar{B}_t}(\theta_2) - \bar{\mathcal{L}}_{2\bar{B}_t}(\theta_2), \text{ where } \bar{\mathcal{L}}_{2\bar{B}_t}(\theta_2) = \sum_{k=1}^K \sum_{\bar{x}_i} (\mathbf{h}_{\pi i} y_{ik} + \frac{1}{m} \text{Lap}(\frac{\Delta_{\mathcal{L}_2}}{\epsilon_2})) W_{\pi k} \quad (12)$$

Theorem 2 *Algorithm 2 preserves $(\epsilon_1/\gamma + \epsilon_2)$ -DP in the optimization of $\bar{\mathcal{L}}_{\bar{B}}(\theta_2)$.*

Since the ϵ_1/γ budget, accumulated from the perturbation of the auto-encoder, is tiny in practice (i.e., $\approx 1e-3$), the additional privacy budget used to preserve DP in the function $\bar{\mathcal{L}}_{\bar{B}_t}(\theta_2)$ can be considered ϵ_2 . We apply the same technique to preserve ϵ_2 -DP in the optimization of the function $\Upsilon(f(\bar{x}_j^{\text{adv}}, \theta_2), y_j)$ over the adversarial examples $\bar{x}_j^{\text{adv}} \in \bar{B}_t^{\text{adv}}$. As the perturbed functions $\bar{\mathcal{L}}$ and $\bar{\Upsilon}$ are always optimized given two disjoint batches \bar{B}_t and \bar{B}_t^{adv} , the privacy budget used to preserve DP in the adversarial objective function $L_{B_t}(\theta_2)$ is ϵ_2 , following the *parallel composition* property in DP [17]. The total budget to learn private parameters $\bar{\theta} = \{\bar{\theta}_1, \bar{\theta}_2\} = \arg \min_{\{\theta_1, \theta_2\}} (\bar{\mathcal{R}}_{B_t}(\theta_1) + \bar{\mathcal{L}}_{B_t}(\theta_2))$ is $(\epsilon_1 + \epsilon_2)$. Similar to other objective function-based approaches [24, 40, 42], the optimization of our mechanism is repeated in T steps, without using additional information from the original data. *It only reads perturbed inputs and perturbed coefficients. In addition, to avoid leaking information about the randomness, generated batches are not changed between epochs (Lines 1 and 5).* Consequently, the privacy budget consumption will not be accumulated at each training step.

Provable Robustness. Now, we establish the correlation between our mechanism and provable robustness. In the *inference time*, to derive the provable robustness condition against adversarial examples $x + \alpha$, i.e., $\forall \alpha \in l_p(1)$, PixelDP mechanism randomizes the scoring function $f(x)$ by injecting *robustness noise* σ_r into either input x or a hidden layer, i.e., $x' = x + \text{Lap}(\frac{\Delta_x}{\epsilon_r})$ or $h' = h + \text{Lap}(\frac{\Delta_h}{\epsilon_r})$, where Δ_x and Δ_h are the sensitivities of x and h , measuring how much x and h can be changed given the perturbation $\alpha \in l_p(1)$ in the input x . Monte Carlo estimation of the expected values $\hat{\mathbb{E}}f(x)$, $\hat{\mathbb{E}}_{lb}f_k(x)$, and $\hat{\mathbb{E}}_{ub}f_k(x)$ are used to derive the robustness condition in Eq. 4.

On the other hand, in our mechanism, the privacy noise σ_p includes Laplace noise injected into both input x , i.e., $\frac{1}{m} \text{Lap}(\frac{\Delta_R}{\epsilon_1})$, and its affine transformation h , i.e., $\frac{2}{m} \text{Lap}(\frac{\Delta_R}{\epsilon_1})$. Note that the perturbation of $\bar{\mathcal{L}}_{2\bar{B}_t}(\theta_2)$ is equivalent to $\bar{\mathcal{L}}_{2\bar{B}_t}(\theta_2) = \sum_{k=1}^K \sum_{\bar{x}_i} (\mathbf{h}_{\pi i} y_{ik} W_{\pi k} + \frac{1}{m} \text{Lap}(\frac{\Delta_{\mathcal{L}_2}}{\epsilon_2})) W_{\pi k}$. This helps us to avoid injecting the noise directly into the coefficients $\mathbf{h}_{\pi i} y_{ik}$. The correlation between our DP preservation and provable robustness lies in the correlation between the privacy noise σ_p and the robustness noise σ_r .

We can derive a robustness bound by projecting the privacy noise σ_p on the scale of the robustness noise σ_r . Given the input x , let $\kappa = \frac{\Delta_R}{m\epsilon_1} / \frac{\Delta_x}{\epsilon_r}$, in our mechanism we have that: $\bar{x} = x + \text{Lap}(\kappa \Delta_x / \epsilon_r)$. By applying a group privacy size κ [17, 38], the scoring function $f(x)$ satisfies ϵ_r -PixelDP given $\alpha \in l_p(\kappa)$, or equivalently is $\kappa \epsilon_r$ -PixelDP given $\alpha \in l_p(1)$, $\delta_r = 0$. By applying Lemma 1, we have

$$\forall k, \forall \alpha \in l_p(\kappa) : \mathbb{E}f_k(x) \leq e^{\epsilon_r} \mathbb{E}f_k(x + \alpha), \text{ or } \forall k, \forall \alpha \in l_p(1) : \mathbb{E}f_k(x) \leq e^{(\kappa \epsilon_r)} \mathbb{E}f_k(x + \alpha) \quad (13)$$

With that, we can achieve a robustness condition against $l_p(\kappa)$ -norm attacks, as follows:

$$\hat{\mathbb{E}}_{lb}f_k(x) > e^{2\epsilon_r} \max_{i:i \neq k} \hat{\mathbb{E}}_{ub}f_i(x) \quad (14)$$

with the probability $\geq \eta_x$ -confidence, derived from the Monte Carlo estimation of $\hat{\mathbb{E}}f(x)$.

Our mechanism also perturbs h (Eq. 8). Given $\varphi = \frac{2\Delta_R}{m\epsilon_1} / \frac{\Delta_h}{\epsilon_r}$, we further have $\bar{h} = h + \text{Lap}(\frac{\varphi \Delta_h}{\epsilon_r})$. Therefore, the scoring function $f(x)$ also satisfies ϵ_r -PixelDP given the perturbation $\alpha \in l_p(\varphi)$. In addition to the robustness to the $l_p(\kappa)$ -norm attacks, we can achieve an additional robustness bound in Eq. 14 against $l_p(\varphi)$ -norm attacks. Similar to PixelDP, these robustness conditions can be achieved as randomization processes in the inference time. They can be considered as *two independent and provable defensive mechanisms* applied against two l_p -norm attacks, i.e., $l_p(\kappa)$ and $l_p(\varphi)$.

One challenging question here is: “What is the general robustness bound, given κ and φ ?” Intuitively, our model is robust to attacks with $\alpha \in l_p(\kappa + \varphi)$. We leverage the theory of *sequential composition* in DP [17] to theoretically answer this question. Given S independent mechanisms $\mathcal{M}_1, \dots, \mathcal{M}_S$,

whose privacy guarantees are $\epsilon_1, \dots, \epsilon_S$ -DP with $\alpha \in l_p(1)$. Each mechanism \mathcal{M}_s , which takes the input x and outputs the value of $f(x)$ with the Laplace noise only injected to randomize the layer s (i.e., no randomization at any other layers), is defined as: $\forall s \in [1, S], \mathcal{M}_s f(x) : \mathbb{R}^d \rightarrow f^s(x) \in \mathbb{R}^K$. We aim to derive a generalized robustness of any composition scoring function $f(\mathcal{M}_1, \dots, \mathcal{M}_S|x)$ bounded in $[0, 1]$, defined as follows:

$$f(\mathcal{M}_1, \dots, \mathcal{M}_S|x) : \prod_{s=1}^S \mathcal{M}_s f(x) \Leftrightarrow f(\mathcal{M}_1, \dots, \mathcal{M}_S|x) : \mathbb{R}^d \rightarrow \prod_{s=1}^S f^s(x) \in \mathbb{R}^K \quad (15)$$

Our setting follows the sequential composition in DP [17]. Thus, we can prove that the expected value $\mathbb{E}f(\mathcal{M}_1, \dots, \mathcal{M}_S|x)$ is insensitive to small perturbations $\alpha \in l_p(1)$, and we derive our composition of robustness, as follows:

Theorem 3 (Composition of Robustness) *Given S independent mechanisms $\mathcal{M}_1, \dots, \mathcal{M}_S$. Given any sequential function $f(\mathcal{M}_1, \dots, \mathcal{M}_S|x)$, and let $\hat{\mathbb{E}}_{lb}$ and $\hat{\mathbb{E}}_{ub}$ are lower and upper bounds with an η -confidence, for the Monte Carlo estimation of $\hat{\mathbb{E}}f(\mathcal{M}_1, \dots, \mathcal{M}_S|x) = \frac{1}{n} \sum_n f(\mathcal{M}_1, \dots, \mathcal{M}_S|x)_n$. For any input x , if $\exists k \in K$ so that*

$$\hat{\mathbb{E}}_{lb} f_k(\mathcal{M}_1, \dots, \mathcal{M}_S|x) > e^{2(\sum_{s=1}^S \epsilon_s)} \max_{i:i \neq k} \hat{\mathbb{E}}_{ub} f_i(\mathcal{M}_1, \dots, \mathcal{M}_S|x), \quad (16)$$

then the predicted label $k = \arg \max_k \hat{\mathbb{E}} f_k(\mathcal{M}_1, \dots, \mathcal{M}_S|x)$, is robust to adversarial examples $x + \alpha$, $\forall \alpha \in l_p(1)$, with probability $\geq \eta$, by satisfying: $\hat{\mathbb{E}} f_k(\mathcal{M}_1, \dots, \mathcal{M}_S|x + \alpha) > \max_{i:i \neq k} \hat{\mathbb{E}} f_i(\mathcal{M}_1, \dots, \mathcal{M}_S|x + \alpha)$, which is the targeted robustness condition in Eq. 2.

To apply the composition of robustness in our mechanism, the noise injections into the input x and its affine transformation h can be considered as two mechanisms \mathcal{M}_x and \mathcal{M}_h , sequentially applied as $(\mathcal{M}_h(x), \mathcal{M}_x(x))$. When $\mathcal{M}_h(x)$ is applied by invoking $f(x)$ with independent draws in the noise χ_2 , the noise χ_1 injected into x is fixed (Lines 3 and 6); and vice-versa. By applying group privacy [17] with sizes κ and φ , the scoring functions $f^x(x)$ and $f^h(x)$, given \mathcal{M}_x and \mathcal{M}_h , are $\kappa\epsilon_r$ -DP and $\varphi\epsilon_r$ -DP given $\alpha \in l_p(1)$. With Theorem 3, we have a generalized robustness bound as follows:

Proposition 1 (DPAL Robustness). *For any input x , if $\exists k \in K : \hat{\mathbb{E}}_{lb} f_k(\mathcal{M}_h, \mathcal{M}_x|x) > e^{2\epsilon_r} \max_{i:i \neq k} \hat{\mathbb{E}}_{ub} f_i(\mathcal{M}_h, \mathcal{M}_x|x)$, then the predicted label k of our function $f(\mathcal{M}_h, \mathcal{M}_x|x)$ is robust to small perturbations $\alpha \in l_p(\kappa + \varphi)$ with the probability $\geq \eta$, by satisfying $\forall \alpha \in l_p(\kappa + \varphi) :$*

$$\hat{\mathbb{E}} f_k(\mathcal{M}_h, \mathcal{M}_x|x + \alpha) > \max_{i:i \neq k} \hat{\mathbb{E}} f_i(\mathcal{M}_h, \mathcal{M}_x|x + \alpha)$$

Training and Verified Inferring. Our model is trained similarly to training typical deep neural networks. Note that we optimize for a *single draw of noise* during training (Line 3). Parameters θ_1 and θ_2 are independently updated by applying gradient descent (Line 15). Regarding the inference time, we implement a *verified inference procedure* as a post-processing step (Lines 16-21). Our verified inference returns a *robustness size guarantee* for each example x , which is the maximal value of $\kappa + \varphi$, for which the robustness condition in Proposition 1 holds. Maximizing $\kappa + \varphi$ is equivalent to maximizing the robustness epsilon ϵ_r , which is the only parameter controlling the size of $\kappa + \varphi$; since, all the other hyper-parameters, i.e., $\Delta_{\mathcal{R}}, m, \epsilon_1, \epsilon_2, \theta_1, \theta_2, \Delta_r^x$, and Δ_r^h are fixed given a well-trained model $f(x)$:

$$(\kappa + \varphi)_{max} = \max_{\epsilon_r} \frac{\Delta_{\mathcal{R}} \epsilon_r}{m \epsilon_1} \left(\frac{1}{\Delta_r^x} + \frac{2}{\Delta_r^h} \right) \text{ s.t. } \hat{\mathbb{E}}_{lb} f_k(x) > e^{2\epsilon_r} \max_{i:i \neq k} \hat{\mathbb{E}}_{ub} f_i(x) \quad (17)$$

The prediction on an example x is robust to attacks up to $(\kappa + \varphi)_{max}$. The failure probability $1-\eta$ can be made arbitrarily small by increasing the number of invocations of $f(x)$, with independent draws in the noise. Similar to [38], Hoeffding's inequality can be applied to bound the approximation error in $\hat{\mathbb{E}} f_k(x)$. We use the following sensitivity bounds $\Delta_r^h = \sqrt{\beta} \|\theta_1\|_\infty$ where $\|\theta_1\|_\infty$ is the maximum 1-norm of θ_1 's rows, and $\Delta_r^x = \mu d^2$. We also propose a new way to draw independent noise following the distribution of $\chi_1 + \frac{1}{m} \text{Lap}(0, \frac{\Delta_{\mathcal{R}}}{\epsilon_1} / \psi)$ for the input x and $2\chi_2 + \frac{2}{m} \text{Lap}(0, \frac{\Delta_{\mathcal{R}}}{\epsilon_1} / \psi)$ for the transformation h , where χ_1 and χ_2 are the fixed noise used to train the network, and ψ is a parameter to control the distribution shifts. This works better without affecting the DP bounds and the robustness. (Details are in **Appendix L**.)

4 Experimental Results

We have carried out an extensive experiment on MNIST and CIFAR-10 datasets. We consider the well-known class of l_∞ bounded adversaries to see whether our mechanism could retain high model utility, while providing strong DP guarantees and protections against adversarial examples, compared with existing mechanisms. Our **DPAL** mechanism is evaluated in comparison with state-of-the-art mechanisms in: (1) DP-preserving algorithms in deep learning, i.e., **DP-SGD** [8], **AdLM** [24], and in (2) Provable robustness, i.e., **PixelDP** [38]. To preserve DP, DP-SGD injects random noise into gradients of parameters, while AdLM is a Functional Mechanism-based approach. PixelDP is one of the state-of-the-art mechanisms providing provable robustness using DP bounds. The baseline models share the same design in our experiment. Four white-box attacks were used, including **FGSM**, **I-FGSM**, Momentum Iterative Method (**MIM**) [43], and **MadryEtAl** [44]. All the models share the same structure, consisting of 2 and 3 convolution layers, respectively for MNIST and CIFAR-10 datasets (detailed configurations are in **Appendix M.1**). We apply two accuracy metrics as follows:

$$\text{conventional acc} = \frac{\sum_{i=1}^{|test|} isCorrect(x_i)}{|test|}; \text{certified acc} = \frac{\sum_{i=1}^{|test|} isCorrect(x_i) \& isRobust(x_i)}{|test|}$$

where $|test|$ is the number of test cases, $isCorrect(\cdot)$ returns 1 if the model makes a correct prediction (else, returns 0), and $isRobust(\cdot)$ returns 1 if the robustness size is larger than a given attack bound μ_a (else, returns 0). **It is important** to note that $x \in [-1, 1]^d$ in our setting, which is different from a common setting $x \in [0, 1]^d$. Thus, the attack size $\mu = 0.3$ in the setting of $x \in [0, 1]^d$ is equivalent to an attack size $2\mu = 0.6$ in our setting. The reason for using $x \in [-1, 1]^d$ is to achieve better model utility, while retaining the same global sensitivities to preserve DP, compared with $x \in [0, 1]^d$. $\epsilon = (\epsilon_1 + \epsilon_2)$ is used to indicate the DP budget used to protect the training data; meanwhile, ϵ_r is the budget for robustness. ϵ_r is set to be 1.0 in the training of our model.

MNIST. Figures 2 and 3 (**Appendix M.2**) illustrate the conventional accuracy of each model as a function of the privacy budget $(\epsilon_1 + \epsilon_2)$ on the MNIST dataset under $l_\infty(\mu_a)$ -norm attacks, with $\mu_a \in \{0.1, 0.2\}$. It is clear that our DPAL outperforms AdLM and DP-SGD, in all cases, i.e., $p < 3e - 10$ (2 tail t-test). AdLM has better accuracies compared with DP-SGD. However, there is no guarantee provided in AdLM. Thus, the accuracy of the AdLM algorithm seems to show no effect against adversarial examples, when the privacy budget is varied. This is different given our DPAL model and the DP-SGD model, whose accuracies are proportional to the privacy budget. Note that when $\mu_a = 0.2$, which is a pretty strong attack, AdLM and DP-SGD become defenseless. By contrast, our model just shows a small drop in terms of accuracy, when μ_a is increased from 0.1 to 0.2, i.e., 1.76% on average, across all attacks and privacy budgets. This illustrates that our mechanism notably enhances the robustness, by incorporating DP into adversarial learning in an ensemble approach.

Figure 6 illustrates the certified accuracy of each model as a function of the adversarial perturbation $\mu_a \in [0.05, 0.6]$. The privacy budget is set to 2.0, offering a reasonable privacy protection. Following [38], in PixelDP, the construction attack bound ϵ_r is set to 0.1, offering a pretty reasonable defense. It is clear that with small perturbations, i.e., $\mu_a \leq 0.2$, PixelDP achieves better certified accuracies under all attacks. This is reasonable, since PixelDP does not preserve DP to protect the training data, compared with our DPAL. Meanwhile, our model outperforms PixelDP when $\mu_a \geq 0.3$, indicating a stronger defense to more aggressive attacks. More importantly, our DPAL has a consistent certified accuracy to different attacks given different perturbation budgets, compared with PixelDP. In fact, when μ_a is increased from 0.05 to 0.6, our DPAL shows a small drop (9.88% in average, from 82.28% ($\mu_a = 0.05$) to 72.40% ($\mu_a = 0.6$)), compared with a huge drop of the PixelDP, i.e., from 94.19% ($\mu_a = 0.05$) to 9.08% ($\mu_a = 0.6$) on average under I-FGSM, MIM, and MadryEtAl attacks, and to 77.47% ($\mu_a = 0.6$) under FGSM attack. This is a promising result.

Our key observations are as follows. **(1)** Incorporating ensemble adversarial learning into DP preservation does enhance the consistency, robustness, and accuracy of our model against different attack algorithms with different levels of perturbations. **(2)** Our DPAL model outperforms baseline algorithms, including both DP-preserving and non-private approaches, in terms of conventional accuracy and certified accuracy in most of the cases.

CIFAR-10. Results on the CIFAR-10 dataset strengthen our observations. In Figures 4 and 5 (**Appendix M.2**), our DPAL clearly outperforms baseline models in all cases, especially when the privacy budget is small (< 6), yielding strong privacy protections. DP-SGD achieves better performance, compared with AdLM. When the privacy budget is increased from 2 to 10, the conventional accuracy

of our DPAL model increases from 44.1% to 48.77%, showing a 4.67% improvement on average. However, the conventional accuracy of our model under adversarial example attacks is still low, i.e., 44.1% on average given the privacy budget at 2.0. This opens a long-term research avenue to achieve better robustness under strong privacy guarantees. The accuracy of our model is also consistent given different attacks with different adversarial perturbations under varied DP protections. Figure 7 also shows that our DPAL model is more accurate than PixelDP ($\epsilon_r = 0.1$) in terms of certified accuracy in all cases, with the privacy budget set to 4.0, offering a reasonable privacy protection.

5 Conclusion

In this paper, we established a connection among DP preservation to protect the training data, adversarial learning, and provable robustness. A sequential composition robustness theory was introduced to generalize robustness given any sequential and bounded function of independent defensive mechanisms. An original DP-preserving mechanism was designed to address the trade-off among model utility, privacy loss, and robustness by tightening the global sensitivity bound. Our model shows promising results and opens a long-term avenue to achieve better robustness under strong privacy guarantees.

References

- [1] M. Fredrikson, S. Jha, and T. Ristenpart, “Model inversion attacks that exploit confidence information and basic countermeasures,” in *Proceedings of the 22Nd ACM SIGSAC Conference on Computer and Communications Security*, ser. CCS ’15, 2015, pp. 1322–1333.
- [2] Y. Wang, C. Si, and X. Wu, “Regression model fitting under differential privacy and model inversion attack,” in *Proceedings of the Twenty-Fourth International Joint Conference on Artificial Intelligence, IJCAI 2015, Buenos Aires, Argentina, July 25-31, 2015*, 2015, pp. 1003–1009.
- [3] R. Shokri, M. Stronati, C. Song, and V. Shmatikov, “Membership inference attacks against machine learning models,” in *2017 IEEE Symposium on Security and Privacy (SP)*, May 2017, pp. 3–18.
- [4] N. Papernot, P. D. McDaniel, A. Sinha, and M. P. Wellman, “Towards the science of security and privacy in machine learning,” *CoRR*, vol. abs/1611.03814, 2016.
- [5] I. J. Goodfellow, J. Shlens, and C. Szegedy, “Explaining and harnessing adversarial examples,” *CoRR*, vol. abs/1412.6572, 2014.
- [6] Y. Liu, X. Chen, C. Liu, and D. Song, “Delving into transferable adversarial examples and black-box attacks,” *CoRR*, vol. abs/1611.02770, 2016.
- [7] N. Carlini and D. Wagner, “Towards evaluating the robustness of neural networks,” in *2017 IEEE Symposium on Security and Privacy (SP)*, May 2017, pp. 39–57.
- [8] M. Abadi, A. Chu, I. Goodfellow, H. B. McMahan, I. Mironov, K. Talwar, and L. Zhang, “Deep learning with differential privacy,” *arXiv:1607.00133*, 2016.
- [9] J. Hamm, J. Luken, and Y. Xie, “Crowd-ml: A library for privacy-preserving machine learning on smart devices,” in *2017 IEEE International Conference on Acoustics, Speech and Signal Processing (ICASSP)*, 2017, pp. 6394–6398.
- [10] N. Kardan and K. O. Stanley, “Mitigating fooling with competitive overcomplete output layer neural networks,” in *2017 International Joint Conference on Neural Networks (IJCNN)*, 2017, pp. 518–525.
- [11] A. Matyasko and L. P. Chau, “Margin maximization for robust classification using deep learning,” in *2017 International Joint Conference on Neural Networks (IJCNN)*, 2017, pp. 300–307.
- [12] Q. Wang, W. Guo, K. Zhang, A. G. O. II, X. Xing, C. L. Giles, and X. Liu, “Learning adversary-resistant deep neural networks,” *CoRR*, vol. abs/1612.01401, 2016.

- [13] M. Cisse, P. Bojanowski, E. Grave, Y. Dauphin, and N. Usunier, “Parseval networks: Improving robustness to adversarial examples,” in *Proceedings of the 34th International Conference on Machine Learning*, ser. Proceedings of Machine Learning Research, D. Precup and Y. W. Teh, Eds., vol. 70, International Convention Centre, Sydney, Australia, 06–11 Aug 2017, pp. 854–863.
- [14] J. Z. Kolter and E. Wong, “Provable defenses against adversarial examples via the convex outer adversarial polytope,” *CoRR*, vol. abs/1711.00851, 2017. [Online]. Available: <http://arxiv.org/abs/1711.00851>
- [15] A. Raghunathan, J. Steinhardt, and P. Liang, “Certified defenses against adversarial examples,” *CoRR*, vol. abs/1801.09344, 2018. [Online]. Available: <http://arxiv.org/abs/1801.09344>
- [16] C. Dwork, F. McSherry, K. Nissim, and A. Smith, “Calibrating noise to sensitivity in private data analysis,” *Theory of Cryptography*, pp. 265–284, 2006.
- [17] C. Dwork and A. Roth, “The algorithmic foundations of differential privacy,” *Found. Trends Theor. Comput. Sci.*, vol. 9, no. 3–4, pp. 211–407, Aug. 2014. [Online]. Available: <http://dx.doi.org/10.1561/04000000042>
- [18] Y. Lecun, L. Bottou, Y. Bengio, and P. Haffner, “Gradient-based learning applied to document recognition,” *Proceedings of the IEEE*, vol. 86, no. 11, pp. 2278–2324, 1998.
- [19] A. Krizhevsky and G. Hinton, “Learning multiple layers of features from tiny images,” 2009.
- [20] K. Chatzikokolakis, M. E. Andrés, N. E. Bordenabe, and C. Palamidessi, “Broadening the scope of differential privacy using metrics,” in *Privacy Enhancing Technologies*, E. De Cristofaro and M. Wright, Eds., 2013, pp. 82–102.
- [21] R. Shokri and V. Shmatikov, “Privacy-preserving deep learning,” in *CCS’15*, 2015, pp. 1310–1321.
- [22] N. Phan, Y. Wang, X. Wu, and D. Dou, “Differential privacy preservation for deep auto-encoders: an application of human behavior prediction,” in *AAAI’16*, 2016, pp. 1309–1316.
- [23] N. Phan, X. Wu, and D. Dou, “Preserving differential privacy in convolutional deep belief networks,” *Machine Learning*, 2017.
- [24] N. Phan, X. Wu, H. Hu, and D. Dou, “Adaptive laplace mechanism: Differential privacy preservation in deep learning,” in *IEEE ICDM’17*, 2017.
- [25] A. Kurakin, I. J. Goodfellow, and S. Bengio, “Adversarial examples in the physical world,” *CoRR*, vol. abs/1607.02533, 2016.
- [26] N. Papernot, P. McDaniel, X. Wu, S. Jha, and A. Swami, “Distillation as a defense to adversarial perturbations against deep neural networks,” in *2016 IEEE Symposium on Security and Privacy (SP)*, May 2016, pp. 582–597.
- [27] N. Papernot, P. McDaniel, S. Jha, M. Fredrikson, Z. B. Celik, and A. Swami, “The limitations of deep learning in adversarial settings,” in *2016 IEEE European Symposium on Security and Privacy*, March 2016, pp. 372–387.
- [28] S. Gu and L. Rigazio, “Towards deep neural network architectures robust to adversarial examples,” *CoRR*, vol. abs/1412.5068, 2014. [Online]. Available: <http://arxiv.org/abs/1412.5068>
- [29] N. Papernot and P. McDaniel, “Extending defensive distillation,” *arXiv preprint arXiv:1705.05264*, 2017.
- [30] H. Hosseini, Y. Chen, S. Kannan, B. Zhang, and R. Poovendran, “Blocking transferability of adversarial examples in black-box learning systems,” *arXiv preprint arXiv:1703.04318*, 2017.
- [31] J. H. Metzen, T. Genewein, V. Fischer, and B. Bischoff, “On detecting adversarial perturbations,” in *Proceedings of 5th International Conference on Learning Representations (ICLR)*, 2017. [Online]. Available: <https://arxiv.org/abs/1702.04267>

- [32] K. Grosse, P. Manoharan, N. Papernot, M. Backes, and P. D. McDaniel, “On the (statistical) detection of adversarial examples,” *CoRR*, vol. abs/1702.06280, 2017. [Online]. Available: <http://arxiv.org/abs/1702.06280>
- [33] W. Xu, D. Evans, and Y. Qi, “Feature squeezing: Detecting adversarial examples in deep neural networks,” *CoRR*, vol. abs/1704.01155, 2017. [Online]. Available: <http://arxiv.org/abs/1704.01155>
- [34] M. Abbasi and C. Gagné, “Robustness to adversarial examples through an ensemble of specialists,” *CoRR*, vol. abs/1702.06856, 2017. [Online]. Available: <http://arxiv.org/abs/1702.06856>
- [35] J. Gao, B. Wang, and Y. Qi, “Deepmask: Masking DNN models for robustness against adversarial samples,” *CoRR*, vol. abs/1702.06763, 2017. [Online]. Available: <http://arxiv.org/abs/1702.06763>
- [36] F. Tramèr, A. Kurakin, N. Papernot, D. Boneh, and P. McDaniel, “Ensemble adversarial training: Attacks and defenses,” *arXiv preprint arXiv:1705.07204*, 2017.
- [37] A. Kurakin, I. J. Goodfellow, and S. Bengio, “Adversarial machine learning at scale,” *CoRR*, vol. abs/1611.01236, 2016.
- [38] M. Lecuyer, V. Atlidakis, R. Geambasu, D. Hsu, and S. Jana, “Certified robustness to adversarial examples with differential privacy,” in *arXiv:1802.03471*, 2018. [Online]. Available: <https://arxiv.org/abs/1802.03471>
- [39] G. Arfken, in *Mathematical Methods for Physicists (Third Edition)*. Academic Press, 1985.
- [40] J. Zhang, Z. Zhang, X. Xiao, Y. Yang, and M. Winslett, “Functional mechanism: regression analysis under differential privacy,” *PVLDB*, vol. 5, no. 11, pp. 1364–1375, 2012.
- [41] Operator norm, “Operator norm,” 2018. [Online]. Available: https://en.wikipedia.org/wiki/Operator_norm
- [42] L. Zhao, Y. Zhang, Q. Wang, Y. Chen, C. Wang, and Q. Zou, “Privacy-preserving collaborative deep learning with irregular participants,” *CoRR*, vol. abs/1812.10113, 2018.
- [43] Y. Dong, F. Liao, T. Pang, X. Hu, and J. Zhu, “Discovering adversarial examples with momentum,” *CoRR*, vol. abs/1710.06081, 2017.
- [44] A. Madry, A. Makelov, L. Schmidt, D. Tsipras, and A. Vladu, “Towards deep learning models resistant to adversarial attacks,” in *International Conference on Learning Representations*, 2018. [Online]. Available: <https://openreview.net/forum?id=rJzIBfZAb>

A Notations and Terminologies

Table 1: Notations and Terminologies.

D and x	Training data with benign examples $x \in [-1, 1]^d$
$y = \{y_1, \dots, y_K\}$	One-hot label vector of K categories
$f : \mathbb{R}^d \rightarrow \mathbb{R}^K$	Function/model f that maps inputs x to a vector of scores $f(x) = \{f_1(x), \dots, f_K(x)\}$
$y_x \in y$	A single true class label of example x
$y(x) = \max_{k \in K} f_k(x)$	Predicted label for the example x given the function f
$x^{\text{adv}} = x + \alpha$	Adversarial example where α is the perturbation
$l_p(\mu) = \{\alpha \in \mathbb{R}^d : \ \alpha\ _p \leq \mu\}$	The l_p -norm ball of attack radius μ
(ϵ_r, δ_r)	Robustness budget ϵ_r and broken probability δ_r
$\mathbb{E}f_k(x)$	The expected value of $f_k(x)$
$\hat{\mathbb{E}}_{lb}$ and $\hat{\mathbb{E}}_{ub}$	Lower and upper bounds of the expected value $\hat{\mathbb{E}}f(x) = \frac{1}{n} \sum_n f(x)_n$
$a(x, \theta_1)$	Feature representation learning model with x and parameters θ_1
B_t	A batch of benign examples x_i
$\mathcal{R}_{B_t}(\theta_1)$	Data reconstruction function given B_t in $a(x, \theta_1)$
$\mathbf{h}_{1B_t} = \{\theta_1^T x_i\}_{x_i \in B_t}$	The values of all hidden neurons in the hidden layer \mathbf{h}_1 of $a(x, \theta_1)$ given the batch B_t
$\tilde{\mathcal{R}}_{B_t}(\theta_1)$ and $\bar{\mathcal{R}}_{B_t}(\theta_1)$	Approximated and perturbed functions of $\mathcal{R}_{B_t}(\theta_1)$
\bar{x}_i and \tilde{x}_i	Perturbed and reconstructed inputs x_i
$\Delta_{\mathcal{R}} = d(\beta + 2)$	Sensitivity of the approximated function $\tilde{\mathcal{R}}_{B_t}(\theta_1)$
$\bar{\mathbf{h}}_{1B_t}$	Perturbed affine transformation \mathbf{h}_{1B_t}
$\bar{x}_j^{\text{adv}} = x_j^{\text{adv}} + \frac{1}{m} \text{Lap}(\frac{\Delta_{\mathcal{R}}}{\epsilon_1})$	DP adversarial examples crafting from benign example x_j
\bar{B}_t and \bar{B}_t^{adv}	Sets of perturbed inputs \bar{x}_i and DP adversarial examples \bar{x}_j^{adv}
$\mathcal{L}_{\bar{B}_t}(\theta_2)$	Loss function of perturbed benign examples in \bar{B}_t , given θ_2
$\Upsilon(f(\bar{x}_j^{\text{adv}}, \theta_2), y_j)$	Loss function of DP adversarial examples \bar{x}_j^{adv} , given θ_2
$\bar{\mathcal{L}}_{\bar{B}_t}(\theta_2)$	DP loss function for perturbed benign examples \bar{B}_t
$\mathcal{L}_{2\bar{B}_t}(\theta_2)$	A part of the loss function $\mathcal{L}_{\bar{B}_t}(\theta_2)$ that needs to be DP
$f(\mathcal{M}_1, \dots, \mathcal{M}_s x)$	Composition scoring function given independent randomizing mechanisms $\mathcal{M}_1, \dots, \mathcal{M}_s$
Δ_r^x and Δ_r^h	Sensitivities of x and h , given the perturbation $\alpha \in l_p(1)$
$(\epsilon_1 + \epsilon_2)$	Privacy budget to protect the training data D
$(\kappa + \varphi)_{\max}$	Robustness size guarantee given an input x at the inference time

B Pseudo-code of Adversarial Training [37]

Given a loss function:

$$L(\theta) = \frac{1}{m_1 + \xi m_2} \left(\sum_{x_i \in B_t} \mathcal{L}(f(x_i, \theta), y_i) + \xi \sum_{x_j^{\text{adv}} \in B_t^{\text{adv}}} \Upsilon(f(x_j^{\text{adv}}, \theta), y_j) \right), \quad (18)$$

where m_1 and m_2 correspondingly are the numbers of examples in B_t and B_t^{adv} at each training step. The typical adversarial learning in [37] is as follows:

Algorithm 1 Adversarial Training [37]

Input: Database D , loss function L , parameters θ , batch sizes m_1 and m_2 , learning rate ϱ_t , and weight control parameter ξ

- 1: **Initialize** θ randomly
 - 2: **for** $t \in [T]$ **do**
 - 3: **Take** a random batch B_t with the size m_1 , and a random batch B_a with the size m_2
 - 4: Craft adversarial examples $B_t^{\text{adv}} = \{x_j^{\text{adv}}\}_{j \in [1, m_2]}$ from corresponding benign examples $x_j \in B_a$
 - 5: **Descent:** $\theta \leftarrow \theta - \varrho_t \nabla_{\theta} L(\theta)$
-

C Pseudo-code of DPAL Mechanism

Algorithm 2 DPAL Mechanism

Input: Database D , loss function L , parameters θ , batch size m , learning rate ϱ_t , privacy budgets: ϵ_1 and ϵ_2 , robustness parameters: ϵ_r , Δ_r^x , and Δ_r^h , adversarial attack size μ_a , the number of invocations n , ensemble attacks A , a parameter ψ , and the size $|\mathbf{h}_\pi|$ of \mathbf{h}_π , and a parameter ξ

- 1: **Randomly Initialize** $\theta = \{\theta_1, \theta_2\}$, $\mathbf{B} = \{B_1, \dots, B_{N/m}\}$ s.t. $\forall B \in \mathbf{B} : B$ is a random batch with the size m , $B_1 \cap \dots \cap B_{N/m} = \emptyset$, and $B_1 \cup \dots \cup B_{N/m} = D$
 - 2: **Construct** a deep neural network f with **hidden layers** $\{\mathbf{h}_1, \dots, \mathbf{h}_\pi\}$, where \mathbf{h}_π is the last hidden layer
 - 3: **Draw Noise** $\chi_1 \leftarrow [Lap(\frac{\Delta_{\mathcal{R}}}{\epsilon_1})]^d$, $\chi_2 \leftarrow [Lap(\frac{\Delta_{\mathcal{R}}}{\epsilon_1})]^\beta$, $\chi_3 \leftarrow [Lap(\frac{\Delta_{\mathcal{L}_2}}{\epsilon_2})]^{|\mathbf{h}_\pi|}$
 - 4: **for** $t \in [T]$ **do**
 - 5: Take a random batch $B_t \in \mathbf{B}$
 - 6: **Perturb** $\forall x_i \in B_t : \bar{x}_i \leftarrow x_i + \frac{\chi_1}{m}; \bar{h}_i \leftarrow h_i + \frac{2\chi_2}{m}$
 - 7: **Assign** $\bar{B}_t \leftarrow \{\bar{x}_i\}_{x_i \in B_t}$
 - 8: **Ensemble DP Adversarial Examples:**
 - 9: **Draw Random Perturbation Value** $\mu_t \in (0, 1]$
 - 10: $\bar{B}_t^{\text{adv}} \leftarrow \emptyset$
 - 11: **for** $i \in A$ **do**
 - 12: **Take** a random batch B_a with the size $m/|A|$
 - 13: $\forall x_j \in B_a$: **Craft** \bar{x}_j^{adv} by using attack algorithm $A[i]$ with $l_\infty(\mu_t)$, $\bar{B}_t^{\text{adv}} \leftarrow \bar{B}_t^{\text{adv}} \cup \bar{x}_j^{\text{adv}}$
 - 14: **Perturb** $L_{B_t}(\theta_2)$ with the noise $\frac{\chi_3}{m}$
 - 15: **Descent:** $\theta_1 \leftarrow \theta_1 - \varrho_t \nabla_{\theta_1} \bar{\mathcal{R}}_{B_t}(\theta_1)$; $\theta_2 \leftarrow \theta_2 - \varrho_t \nabla_{\theta_2} \bar{L}_{B_t}(\theta_2)$
 - 16: **Output:** $(\epsilon_1 + \epsilon_2)$ -DP parameters $\theta = \{\theta_1, \theta_2\}$, robust model with an ϵ_r budget
 - 17: **Verified Inferring:** (an input x , attack size μ_a)
 - 18: **Compute** robustness size $(\kappa + \varphi)_{\max}$ in Eq. 17 of x
 - 19: **if** $(\kappa + \varphi)_{\max} \geq \mu$ **then**
 - 20: **Return** $isRobust(x) = True$, label k , $(\kappa + \varphi)_{\max}$
 - 21: **else**
 - 22: **Return** $isRobust(x) = False$, label k , $(\kappa + \varphi)_{\max}$
-

D Proof of Lemma 2

Inspired by the proof of *Functional Mechanism* [40], we have our proof as follows:

Proof 1 Assume that B_t and B'_t differ in the last tuple, x_m (x'_m). Then,

$$\begin{aligned} \Delta_{\mathcal{R}} &= \sum_{j=1}^d \left[\left\| \sum_{x_i \in B_t} \frac{1}{2} h_i - \sum_{x'_i \in B'_t} \frac{1}{2} h'_i \right\|_1 + \left\| \sum_{x_i \in B_t} x_{ij} - \sum_{x'_i \in B'_t} x'_{ij} \right\|_1 \right] \\ &\leq 2 \max_{x_i} \sum_{j=1}^d \left(\left\| \frac{1}{2} h_i \right\|_1 + \|x_{ij}\|_1 \right) \leq d(\beta + 2) \end{aligned}$$

E Proof of Lemma 1

Inspired by the proof of *Functional Mechanism* [40], we have our proof as follows:

Proof 2 Given χ_1 drawn as a Laplace noise $[Lap(\frac{\Delta_{\mathcal{R}}}{\epsilon_1})]^d$ and χ_2 drawn as a Laplace noise $[Lap(\frac{\Delta_{\mathcal{R}}}{\epsilon_1})]^\beta$, the perturbation of the coefficient $\phi \in \Phi = \{\frac{1}{2} h_i, x_i\}$, denoted as $\bar{\phi}$, can be rewritten

as follows:

$$\text{for } \phi \in \{x_i\} : \bar{\phi} = \sum_{x_i \in B} (\phi_{x_i} + \frac{\chi_1}{m}) = \sum_{x_i \in B} \phi_{x_i} + \chi_1 = \sum_{x_i \in B} \phi_{x_i} + [Lap(\frac{\Delta_{\mathcal{R}}}{\epsilon_1})]^d$$

$$\text{for } \phi \in \{\frac{1}{2}h_i\} : \bar{\phi} = \sum_{x_i \in B} \frac{1}{2}(h_i + \frac{2\chi_2}{m}) = \sum_{x_i \in B} (\phi_{x_i} + \frac{\chi_2}{m}) = \sum_{x_i \in B} \phi_{x_i} + \chi_2 = \sum_{x_i \in B} \phi_{x_i} + [Lap(\frac{\Delta_{\mathcal{R}}}{\epsilon_1})]^\beta$$

we have

$$Pr(\bar{\mathcal{R}}_{B_t}(\theta_1)) = \prod_{j=1}^d \prod_{\phi \in \Phi} \exp\left(-\frac{\epsilon_1 \|\sum_{x_i \in B} \phi_{x_i} - \bar{\phi}\|_1}{\Delta_{\mathcal{R}}}\right)$$

$\Delta_{\mathcal{R}}$ is set to $d(\beta + 2)$, we have that:

$$\begin{aligned} \frac{Pr(\bar{\mathcal{R}}_{B_t}(\theta_1))}{Pr(\bar{\mathcal{R}}_{B'_t}(\theta_1))} &= \frac{\prod_{j=1}^d \prod_{\phi \in \Phi} \exp\left(-\frac{\epsilon_1 \|\sum_{x_i \in B_t} \phi_{x_i} - \bar{\phi}\|_1}{\Delta_{\mathcal{R}}}\right)}{\prod_{j=1}^d \prod_{\phi \in \Phi} \exp\left(-\frac{\epsilon_1 \|\sum_{x'_i \in B'_t} \phi_{x'_i} - \bar{\phi}\|_1}{\Delta_{\mathcal{R}}}\right)} \\ &\leq \prod_{j=1}^d \prod_{\phi \in \Phi} \exp\left(\frac{\epsilon_1}{\Delta_{\mathcal{R}}} \left\| \sum_{x_i \in B_t} \phi_{x_i} - \sum_{x'_i \in B'_t} \phi_{x'_i} \right\|_1\right) \\ &\leq \prod_{j=1}^d \prod_{\phi \in \Phi} \exp\left(\frac{\epsilon_1}{\Delta_{\mathcal{R}}} 2 \max_{x_i \in B_t} \|\phi_{x_i}\|_1\right) \leq \exp\left(\frac{\epsilon_1 d(\beta + 2)}{\Delta_{\mathcal{R}}}\right) \\ &= \exp(\epsilon_1) \end{aligned}$$

Consequently, the computation of $\bar{\mathcal{R}}_{B_t}(\theta_1)$ preserves ϵ_1 -DP in Alg. 2. In addition, the parameter optimization of $\bar{\mathcal{R}}_{B_t}(\theta_1)$ only uses the perturbed data \bar{x}_i in the computations of h_i , \bar{h}_i , and \tilde{x}_i . Thus, the perturbed optimal parameters $\bar{\theta}_1$ is ϵ_1 -DP.

F Proof of Lemma 3

Proof 3 Regarding the computation of $\mathbf{h}_{1B_t} = \{\bar{\theta}_1^T \bar{x}_i\}_{x_i \in B_t}$, we can see that $h_i = \bar{\theta}_1^T \bar{x}_i$ is a linear function of x . The sensitivity of a function h is defined as the maximum change in output, that can be generated by a change in the input [38]. Therefore, the global sensitivity of \mathbf{h}_1 can be computed as follows:

$$\begin{aligned} \Delta_{\mathbf{h}_1} &= \frac{\|\sum_{x_i \in B_t} \bar{\theta}_1^T \bar{x}_i - \sum_{x'_i \in B'_t} \bar{\theta}_1^T \bar{x}'_i\|_1}{\|\sum_{x_i \in B_t} \bar{x}_i - \sum_{x'_i \in B'_t} \bar{x}'_i\|_1} \\ &\leq \max_{x_i \in B_t} \frac{\|\bar{\theta}_1^T \bar{x}_i\|_1}{\|\bar{x}_i\|_1} \leq \|\bar{\theta}_1^T\|_{1,1} \end{aligned}$$

following matrix norms [41]: $\|\bar{\theta}_1^T\|_{1,1}$ is the maximum 1-norm of θ_1 's columns. By injecting Laplace noise $Lap(\frac{\Delta_{\mathbf{h}_1}}{\epsilon_1})$ into \mathbf{h}_{1B_t} , i.e., $\mathbf{h}_{1B_t} = \{\bar{\theta}_1^T \bar{x}_i + Lap(\frac{\Delta_{\mathbf{h}_1}}{\epsilon_1})\}_{x_i \in B_t}$, we can preserve ϵ_1 -DP in the computation of \mathbf{h}_{1B_t} . Let us set $\Delta_{\mathbf{h}_1} = \|\bar{\theta}_1^T\|_{1,1}$, $\gamma = \frac{2\Delta_{\mathcal{R}}}{m\Delta_{\mathbf{h}_1}}$, and χ_2 drawn as a Laplace noise $[Lap(\frac{\Delta_{\mathcal{R}}}{\epsilon_1})]^\beta$, in our mechanism, the perturbed affine transformation $\bar{\mathbf{h}}_{1B_t}$ is presented as:

$$\begin{aligned} \bar{\mathbf{h}}_{1B_t} &= \{\bar{\theta}_1^T \bar{x}_i + \frac{2\chi_2}{m}\}_{x_i \in B_t} = \{\bar{\theta}_1^T \bar{x}_i + \frac{2}{m}[Lap(\frac{\Delta_{\mathcal{R}}}{\epsilon_1})]^\beta\}_{x_i \in B_t} \\ &= \{\bar{\theta}_1^T \bar{x}_i + [Lap(\frac{\gamma\Delta_{\mathbf{h}_1}}{\epsilon_1})]^\beta\}_{x_i \in B_t} \\ &= \{\bar{\theta}_1^T \bar{x}_i + [Lap(\frac{\Delta_{\mathbf{h}_1}}{\epsilon_1/\gamma})]^\beta\}_{x_i \in B_t} \end{aligned}$$

This results in an (ϵ_1/γ) -DP affine transformation $\bar{\mathbf{h}}_{1B_t} = \{\bar{\theta}_1^T \bar{x}_i + [Lap(\frac{\Delta_{\mathbf{h}_1}}{\epsilon_1/\gamma})]^\beta\}_{x_i \in B_t}$. Therefore, Lemma 3 does hold.

G Proof of Lemma 4

Proof 4 Assume that \bar{B}_t and \bar{B}'_t differ in the last tuple, and \bar{x}_m (\bar{x}'_m) be the last tuple in \bar{B}_t (\bar{B}'_t), we have that

$$\begin{aligned}\Delta_{\mathcal{L}2} &= \sum_{k=1}^K \left\| \sum_{\bar{x}_i \in \bar{B}_t} (\mathbf{h}_{\pi i} y_{ik}) - \sum_{\bar{x}'_i \in \bar{B}'_t} (\mathbf{h}'_{\pi i} y'_{ik}) \right\|_1 \\ &= \sum_{k=1}^K \left\| \mathbf{h}_{\pi m} y_{mk} - \mathbf{h}'_{\pi m} y'_{mk} \right\|_1\end{aligned}$$

Since y_{mk} and y'_{mk} are one-hot encoding, we have that $\Delta_{\mathcal{L}2} \leq 2 \max_{\bar{x}_i} \|\mathbf{h}_{\pi i}\|_1$. Given $\mathbf{h}_{\pi i} \in [-1, 1]$, we have

$$\Delta_{\mathcal{L}2} \leq 2|\mathbf{h}_{\pi}| \quad (19)$$

Lemma 4 does hold.

H Proof of Lemma 2

Proof 5 Let \bar{B}_t and \bar{B}'_t be neighboring batches of benign examples, and χ_3 drawn as Laplace noise $[Lap(\frac{\Delta_{\mathcal{L}2}}{\epsilon_2})]^{|\mathbf{h}_{\pi}|}$, the perturbations of the coefficients $\mathbf{h}_{\pi i} y_{ik}$ can be rewritten as:

$$\bar{\mathbf{h}}_{\pi i} \bar{y}_{ik} = \sum_{\bar{x}_i} (\mathbf{h}_{\pi i} y_{ik} + \frac{\chi_3}{m}) = \sum_{\bar{x}_i} (\mathbf{h}_{\pi i} y_{ik}) + [Lap(\frac{\Delta_{\mathcal{L}2}}{\epsilon_2})]^{|\mathbf{h}_{\pi}|}$$

Since all the coefficients are perturbed, and given $\Delta_{\mathcal{L}2} = 2|\mathbf{h}_{\pi}|$, we have that

$$\begin{aligned}\frac{Pr(\mathcal{L}_{\bar{B}_t}(\theta_2))}{Pr(\mathcal{L}_{\bar{B}'_t}(\theta_2))} &= \frac{Pr(\mathcal{L}_{1\bar{B}_t}(\theta_2))}{Pr(\mathcal{L}_{1\bar{B}'_t}(\theta_2))} \times \frac{Pr(\bar{\mathcal{L}}_{2\bar{B}_t}(\theta_2))}{Pr(\bar{\mathcal{L}}_{2\bar{B}'_t}(\theta_2))} \\ &\leq e^{\epsilon_1/\gamma} \sum_{k=1}^K \frac{\exp(-\frac{\epsilon_2 \|\sum_{\bar{x}_i} \mathbf{h}_{\pi i} y_{ik} - \bar{\mathbf{h}}_{\pi i} \bar{y}_{ik}\|_1}{\Delta_{\mathcal{L}2}})}{\exp(-\frac{\epsilon_2 \|\sum_{\bar{x}'_i} \mathbf{h}_{\pi i} y_{ik} - \bar{\mathbf{h}}_{\pi i} \bar{y}_{ik}\|_1}{\Delta_{\mathcal{L}2}})} \\ &\leq e^{\epsilon_1/\gamma} \sum_{k=1}^K \exp(\frac{\epsilon_2}{\Delta_{\mathcal{L}2}} \left\| \sum_{\bar{x}_i} \mathbf{h}_{\pi i} y_{ik} - \sum_{\bar{x}'_i} \mathbf{h}_{\pi i} y_{ik} \right\|_1) \\ &\leq e^{\epsilon_1/\gamma} \exp(\frac{\epsilon_2}{\Delta_{\mathcal{L}2}} 2 \max_{\bar{x}_i} \|\mathbf{h}_{\pi i}\|_1) = e^{\epsilon_1/\gamma + \epsilon_2}\end{aligned}$$

The computation of $\bar{\mathcal{L}}_{2\bar{B}_t}(\theta_2)$ preserves $(\epsilon_1/\gamma + \epsilon_2)$ -differential privacy. The optimization of $\bar{\mathcal{L}}_{2\bar{B}_t}(\theta_2)$ does not access additional information from the original input $x_i \in B$. Consequently, the optimal perturbed parameters $\bar{\theta}_2$ derived from $\bar{\mathcal{L}}_{2\bar{B}_t}(\theta_2)$ are $(\epsilon_1/\gamma + \epsilon_2)$ -DP.

I Proof of Lemma 5

Lemma 5 Given S independent mechanisms $\mathcal{M}_1, \dots, \mathcal{M}_S$, which are $\epsilon_1, \dots, \epsilon_S$ -DP w.r.t a l_p -norm metric, then the expected output value of any sequential function f of them, i.e., $f(\mathcal{M}_1, \dots, \mathcal{M}_S|x)$, with bounded output $f(\mathcal{M}_1, \dots, \mathcal{M}_S|x) \in [0, 1]$, meets the following property: $\forall \alpha \in l_p(1)$:

$$\mathbb{E}f(\mathcal{M}_1, \dots, \mathcal{M}_S|x) \leq e^{(\sum_{s=1}^S \epsilon_s)} \mathbb{E}f(\mathcal{M}_1, \dots, \mathcal{M}_S|x + \alpha)$$

Proof 6 Thanks to the sequential composition theory in DP [17], $f(\mathcal{M}_1, \dots, \mathcal{M}_S|x)$ is $(\sum_s \epsilon_s)$ -DP, since for any $O = \prod_{s=1}^S o_s \in \prod_{s=1}^S f^s(x) (\in \mathbb{R}^K)$, we have that

$$\begin{aligned}\frac{P(f(\mathcal{M}_1, \dots, \mathcal{M}_S|x) = O)}{P(f(\mathcal{M}_1, \dots, \mathcal{M}_S|x + \alpha) = O)} &= \frac{P(\mathcal{M}_1 f(x) = o_1) \dots P(\mathcal{M}_S f(x) = o_S)}{P(\mathcal{M}_1 f(x + \alpha) = o_1) \dots P(\mathcal{M}_S f(x + \alpha) = o_S)} \\ &\leq \prod_{s=1}^S \exp(\epsilon_s) = e^{(\sum_{s=1}^S \epsilon_s)}\end{aligned}$$

As a result, we have

$$P(f(\mathcal{M}_1, \dots, \mathcal{M}_S|x)) \leq e^{(\sum_i \epsilon_i)} P(f(\mathcal{M}_1, \dots, \mathcal{M}_S|x + \alpha))$$

The sequential composition of the expected output is as:

$$\begin{aligned} \mathbb{E}f(\mathcal{M}_1, \dots, \mathcal{M}_S|x) &= \int_0^1 P(f(\mathcal{M}_1, \dots, \mathcal{M}_S|x) > t) dt \\ &\leq e^{(\sum_s \epsilon_s)} \int_0^1 P(f(\mathcal{M}_1, \dots, \mathcal{M}_S|x + \alpha) > t) dt \\ &= e^{(\sum_s \epsilon_s)} \mathbb{E}f(\mathcal{M}_1, \dots, \mathcal{M}_S|x + \alpha) \end{aligned}$$

Lemma 5 does hold.

J Proof of Theorem 3

Proof 7 $\forall \alpha \in l_p(1)$, from Lemma 5, with probability $\geq \eta$, we have that

$$\begin{aligned} \hat{\mathbb{E}}f_k(\mathcal{M}_1, \dots, \mathcal{M}_S|x + \alpha) &\geq \frac{\hat{\mathbb{E}}f_k(\mathcal{M}_1, \dots, \mathcal{M}_S|x)}{e^{(\sum_{s=1}^S \epsilon_s)}} \\ &\geq \frac{\hat{\mathbb{E}}_{lb}f_k(\mathcal{M}_1, \dots, \mathcal{M}_S|x)}{e^{(\sum_{s=1}^S \epsilon_s)}} \end{aligned} \quad (20)$$

In addition, we also have

$$\begin{aligned} \forall i \neq k : \hat{\mathbb{E}}f_{i:i \neq k}(\mathcal{M}_1, \dots, \mathcal{M}_S|x + \alpha) &\leq e^{(\sum_{s=1}^S \epsilon_s)} \hat{\mathbb{E}}f_{i:i \neq k}(\mathcal{M}_1, \dots, \mathcal{M}_S|x) \\ \Rightarrow \forall i \neq k : \hat{\mathbb{E}}f_i(\mathcal{M}_1, \dots, \mathcal{M}_S|x + \alpha) &\leq e^{(\sum_{s=1}^S \epsilon_s)} \max_{i:i \neq k} \hat{\mathbb{E}}_{ub}f_i(\mathcal{M}_1, \dots, \mathcal{M}_S|x) \end{aligned} \quad (21)$$

Using the hypothesis (Eq. 16) and the first inequality (Eq. 20), we have that

$$\begin{aligned} \hat{\mathbb{E}}f_k(\mathcal{M}_1, \dots, \mathcal{M}_S|x + \alpha) &> \frac{e^{2(\sum_{s=1}^S \epsilon_s)} \max_{i:i \neq k} \hat{\mathbb{E}}_{ub}f_i(\mathcal{M}_1, \dots, \mathcal{M}_S|x)}{e^{(\sum_{s=1}^S \epsilon_s)}} \\ &> e^{(\sum_{s=1}^S \epsilon_s)} \max_{i:i \neq k} \hat{\mathbb{E}}_{ub}f_i(\mathcal{M}_1, \dots, \mathcal{M}_S|x) \end{aligned}$$

Now, we apply the third inequality (Eq. 21), we have that

$$\begin{aligned} \forall i \neq k : \hat{\mathbb{E}}f_k(\mathcal{M}_1, \dots, \mathcal{M}_S|x + \alpha) &> \hat{\mathbb{E}}f_i(\mathcal{M}_1, \dots, \mathcal{M}_S|x + \alpha) \\ \Leftrightarrow \hat{\mathbb{E}}f_k(\mathcal{M}_1, \dots, \mathcal{M}_S|x + \alpha) &> \max_{i:i \neq k} \hat{\mathbb{E}}f_i(\mathcal{M}_1, \dots, \mathcal{M}_S|x + \alpha) \end{aligned}$$

The Theorem 3 does hold.

K Proof of Proposition 1

Proof 8 $\forall \alpha \in l_p(1)$, by applying Theorem 3, we have

$$\begin{aligned} \hat{\mathbb{E}}_{lb}f_k(\mathcal{M}_h, \mathcal{M}_x|x) &> e^{2(\kappa\epsilon_r + \varphi\epsilon_r)} \max_{i:i \neq k} \hat{\mathbb{E}}_{ub}f_i(\mathcal{M}_h, \mathcal{M}_x|x) \\ &> e^{2(\kappa + \varphi)\epsilon_r} \max_{i:i \neq k} \hat{\mathbb{E}}_{ub}f_i(\mathcal{M}_h, \mathcal{M}_x|x) \end{aligned}$$

Furthermore, by applying group privacy, we have that

$$\forall \alpha \in l_p(\kappa + \varphi) : \hat{\mathbb{E}}_{lb}f_k(\mathcal{M}_h, \mathcal{M}_x|x) > e^{2\epsilon_r} \max_{i:i \neq k} \hat{\mathbb{E}}_{ub}f_i(\mathcal{M}_h, \mathcal{M}_x|x)$$

By applying Proof 7, it is straight to have

$$\forall \alpha \in l_p(\kappa + \varphi) : \hat{\mathbb{E}}f_k(\mathcal{M}_h, \mathcal{M}_x|x + \alpha) > \max_{i:i \neq k} \hat{\mathbb{E}}f_k(\mathcal{M}_h, \mathcal{M}_x|x + \alpha)$$

with probability $\geq \eta$. Proposition 1 does hold.

L Monte Carlo Estimation of $\hat{\mathbb{E}}f(x)$

Recall that the Monte Carlo estimation is applied to estimate the expected value $\hat{\mathbb{E}}f(x) = \frac{1}{n} \sum_n f(x)_n$, where n is the number of invocations of $f(x)$ with independent draws in the noise, i.e., $\frac{1}{m} \text{Lap}(0, \frac{\Delta_R}{\epsilon_1})$ and $\frac{2}{m} \text{Lap}(0, \frac{\Delta_R}{\epsilon_1})$ in our case. When ϵ_1 is small (indicating a strong privacy protection), it causes a *notably large distribution shift among independent draws of the Laplace noise*. In addition, let us denote a single draw in the noise as $\chi_1 = \frac{1}{m} \text{Lap}(0, \frac{\Delta_R}{\epsilon_1})$ used to train the scoring function $f(x)$, the model converges to the point that the noise χ_1 and $2\chi_1$ need to be correspondingly added into x and h in order to make correct predictions. χ_1 can be approximated as $\text{Lap}(\chi_1, \varrho)$, where $\varrho \rightarrow 0$. It is clear to see that independent draws of the noise $\frac{1}{m} \text{Lap}(0, \frac{\Delta_R}{\epsilon_1})$ have *distribution shifts* with the fixed noise $\chi_1 \approx \text{Lap}(\chi_1, \varrho)$. These distribution shifts can also be large, when noise is large. We have experienced that these distribution shifts in having independent draws of noise to estimate $\hat{\mathbb{E}}f(x)$ can notably degrade the inference accuracy of the scoring function, when privacy budget ϵ_1 is small resulting in a large amount of noise injected to provide strong privacy guarantees.

To address this problem, one solution is to increase the number of invocations of $f(x)$, i.e., n , to a huge number per prediction. This is impractical in real-world scenarios. We propose a novel way to draw independent noise following the distribution of $\chi_1 + \frac{1}{m} \text{Lap}(0, \frac{\Delta_R}{\epsilon_1}/\psi)$ for the input x and $2\chi_1 + \frac{2}{m} \text{Lap}(0, \frac{\Delta_R}{\epsilon_1}/\psi)$ for the affine transformation h , where ψ is a hyper-parameter to control the distribution shifts. This approach works well and does not affect the DP bounds and the provable robustness condition, since: **(1)** Our mechanism achieves both DP and provable robustness in the training process; and **(2)** It is clear that $\hat{\mathbb{E}}f(x) = \frac{1}{n} \sum_n f(x)_n = \frac{1}{n} \sum_n g(a(x + \chi_1 + \frac{1}{m} \text{Lap}_n(0, \frac{\Delta_R}{\epsilon_1}/\psi), \theta_1) + 2\chi_1 + \frac{2}{m} \text{Lap}_n(0, \frac{\Delta_R}{\epsilon_1}/\psi), \theta_2)$, where $\text{Lap}_n(0, \frac{\Delta_R}{\epsilon_1}/\psi)$ is the n -th draw of the noise. When $n \rightarrow \infty$, $\hat{\mathbb{E}}f(x)$ will converge to $\frac{1}{n} \sum_n g(a(x + \chi_1, \theta_1) + 2\chi_1, \theta_2)$, which aligns well with the convergence point of the scoring function $f(x)$. Injecting χ_1 and $2\chi_1$ to x and h during the estimation of $\hat{\mathbb{E}}f(x)$ yields better performance, without affecting the DP bounds and the provable robustness condition.

M Supplemental Experimental Results

M.1 Model Configuration

The MNIST database of handwritten digits [18]. Each example is a 28×28 size gray-level image. The CIFAR-10 dataset consists of color images belonging to 10 classes, i.e., airplanes, dogs, etc. The dataset is splitted into 50,000 training samples and 10,000 test samples [19].

MNIST: We used two convolution layers (32 and 64 features). Each hidden neuron connects with a 5×5 unit patch. A fully-connected layer has 256 units. The batch size m was set to 2,400, $\xi = 1.5$, $\psi = 2$. I-FGSM, MIM, and MadryEtAl were used to draft $l_\infty(\mu)$ adversarial examples in training, with $T_\mu = 10$. **CIFAR-10:** We used three convolution layers (128, 128, and 256 features). Each hidden neuron connects with a 3×3 unit patch in the first layer, and a 5×5 unit patch in other layers. One fully-connected layer has 256 neurons. The batch size m was set to 1,800, $\xi = 1.5$, $\psi = 10$, and $T_\mu = 3$. The ensemble of attack algorithms \mathcal{A} includes I-FGSM, MIM, and MadryEtAl. We do use data augmentation, including random crop, random flip, and random contrast. The implementation of our mechanism is available in TensorFlow. The experiments were conducted on a single GPU, i.e., NVIDIA GTX TITAN X, 12 GB with 3,072 CUDA cores.

To select the best hyper-parameters, including $\xi \in [1, 6]$ and $\psi \in [1, 10]$, for each dataset, we varied the privacy budget $(\epsilon_1 + \epsilon_2)$ and the attack size μ_a , given each value of ξ and ψ , i.e., $(\epsilon_1 + \epsilon_2) \in [0.2, 2]$ in MNIST dataset, $(\epsilon_1 + \epsilon_2) \in [2, 10]$ in CIFAR-10 dataset, and $\mu_a \in [0.05, 0.6]$ for both datasets. Each setting is executed 3 times; resulting in 105 runs in total for each value of ξ and ψ . The average accuracies were used to identify the best values of ξ and ψ for both datasets. Then, the best values were used to conduct our experiments (Figures 2-7). Each setting of each algorithm was executed 7 times, and the average results were reported. Learning rate ϱ_t was set to $1e - 4$.

M.2 Complete Experimental Results

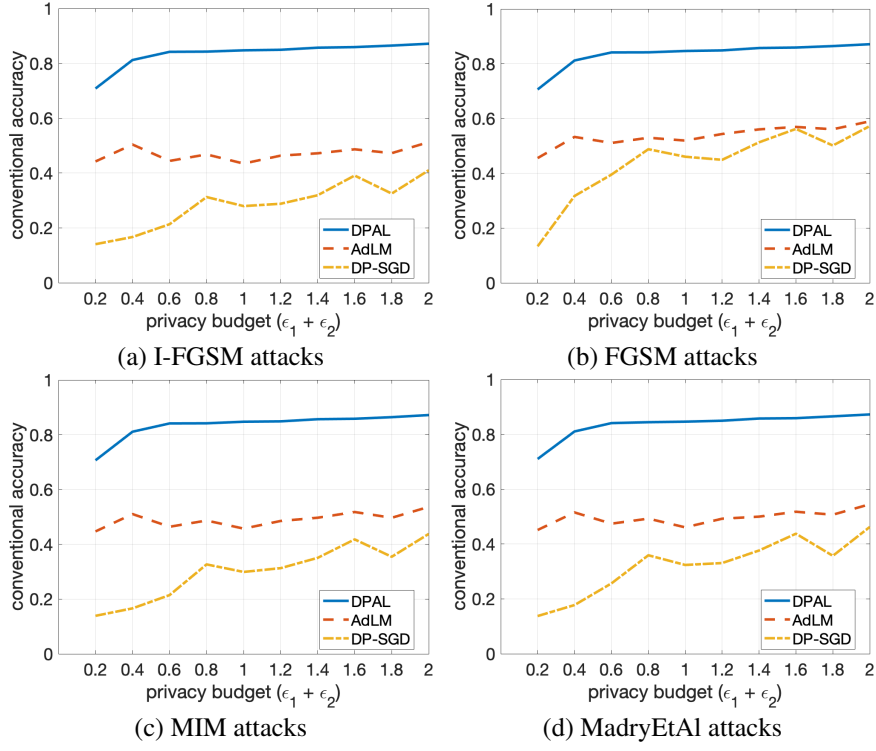


Figure 2: Conventional accuracy on the MNIST dataset, under $l_\infty(\mu_a = 0.1)$.

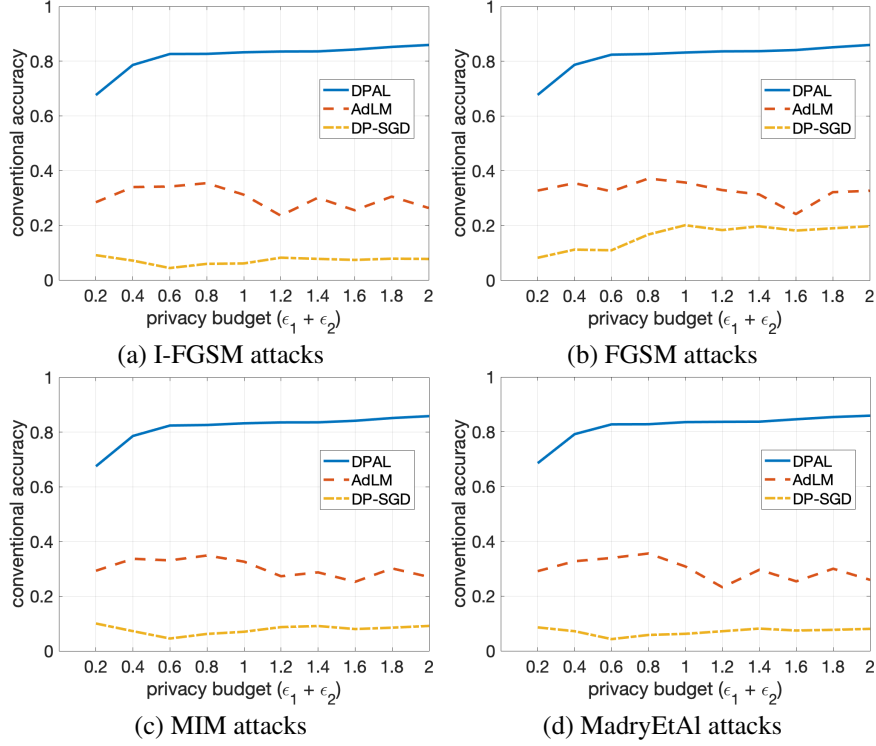


Figure 3: Conventional accuracy on the MNIST dataset, under $l_\infty(\mu_a = 0.2)$.

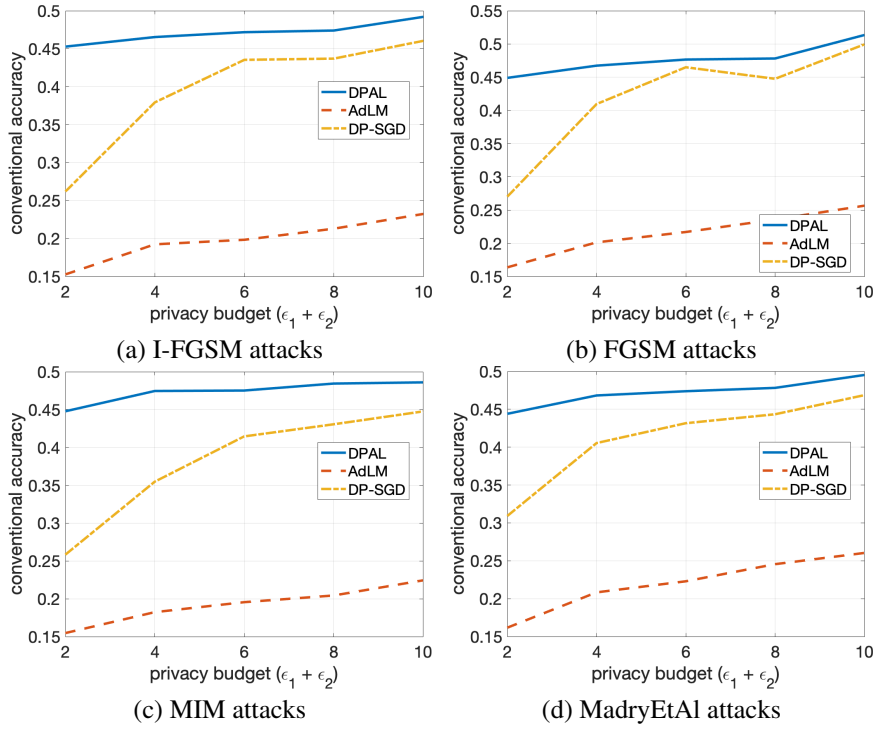


Figure 4: Conventional accuracy on the CIFAR-10 dataset, given $l_\infty(\mu_a = 0.1)$.

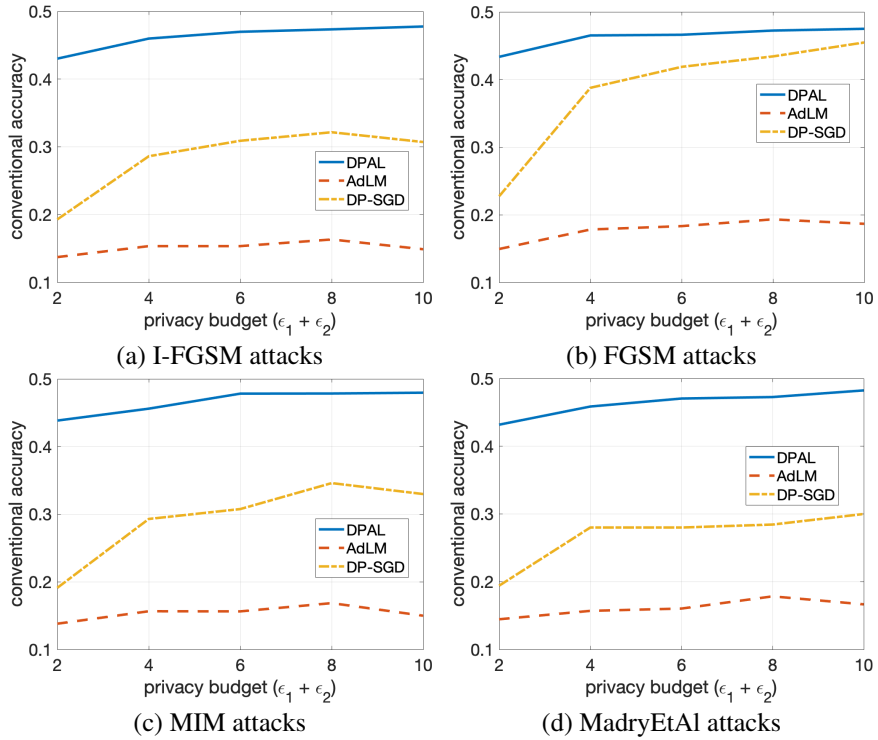


Figure 5: Conventional accuracy on the CIFAR-10 dataset, given $l_\infty(\mu_a = 0.2)$.

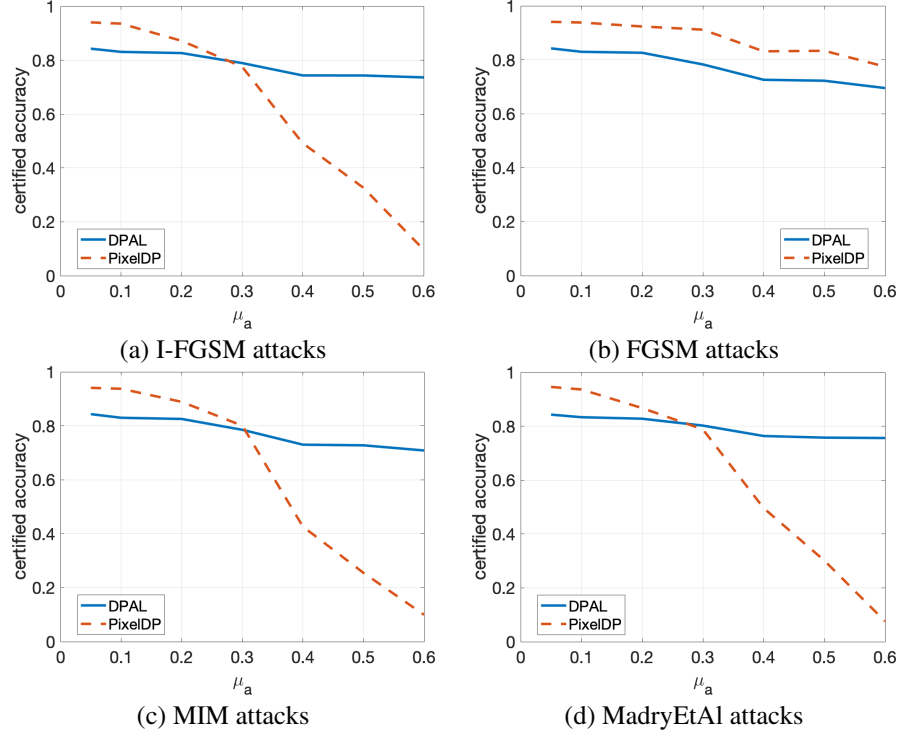


Figure 6: Certified accuracy on the MNIST dataset. The privacy budget is set to 2, offering a reasonable privacy protection.

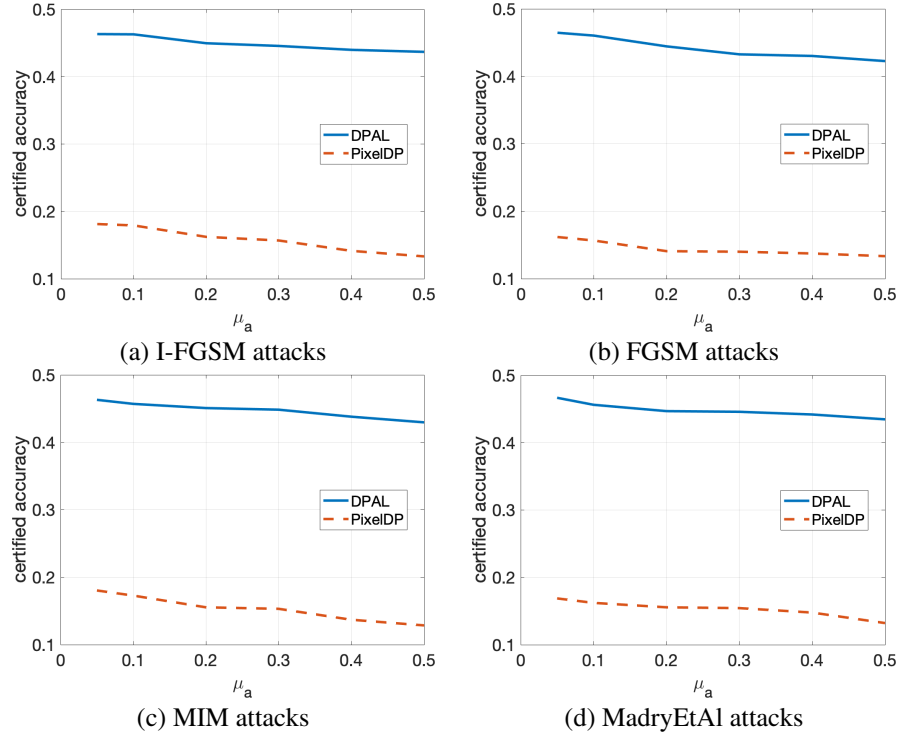


Figure 7: Certified accuracy on the CIFAR-10 dataset. The privacy budget is set to 4, offering a reasonable privacy protection.